PERFORMANCE PREDICTION OF MULTISTAGE AXIAL-FLOW TURBOMACHINES

By
N. SITARAM

DEPARTMENT OF AERONAUTICAL ENGINEERING
INDIAN INSTITUTE OF TECHNOLOGY KANPUR
SEPTEMBER, 1975

PERFORMANCE PREDICTION OF MULTISTAGE AXIAL-FLOW TURBOMACHINES

A Thesis Submitted
in partial Fulfilment of the Requirements
for the Degree of
MASTER OF TECHNOLOGY

By
N. SITARAM

to the

DEPARTMENT OF AERONAUTICAL ENGINEERING
INDIAN INSTITUTE OF TECHNOLOGY KANPUR
SEPTEMBER, 1975

CERTIFICATE

This is to certify that the thesis entitled "Performance Prediction of Multi-stage Axial Flow Turbomachines" by N. Sitaram is a record of work carried out under our joint supervision and has not been submitted elsewhere for a degree.

(C.S. Moorthy)
Professor
Dept. of Aero. Engg.
I.I.T. Kanpur

(Ramiyar Singh)
Assistant Professor
Dept. of Mech. Engg.
I.I.T. Kanpur

ABSTRACT

Theoretical performance of multistage axial-flow turbomachines is determined using the streamline curvature method. The mathematical model is based on that developed by Moorthy[7]. The flow field equations are solved numerically on a computer. Input to the program consists of annulus geometry, design fluid angles, a polytropic coefficient to account for losses at each operating point and inlet conditions to the turbomachine.

The radial equilibrium equation (r.e.e.) along with continuity equation and auxiliary equations is solved in the inter blade row gaps using finite difference technique. The output consists of radial distribution of flow parameters, overall pressure ratio and adiabatic efficiency as a function of mass flow and rotational speed. These results are compared with experimental results, whenever available.

CONTENTS

		Page
NOMENCLATURE		v
CHAPTER I :	INTRODUCTION	
I.A :	General Background	1
I.B :	Review of Previous Work	4
CHAPTER II. :	FORMULATION OF THE PROBLEM	
II.A :	Preliminary Considerations	8
II.B :	Assumptions	9
II.C :	Derivation of Radial Equilibrium Equation	10
II.D :	Auxiliary Equations	15
II.E :	Estimation of Fluid Angles At Off-Design Conditions	18
CHAPTER III :	METHOD OF SOLUTION	
III.A :	Finite Difference Equations	20
III.B :	Solution of Finite-Difference Equations	23
III.C :	Numerical Difficulties and Their Elimination	28
CHAPTER IV :	RESULTS AND DISCUSSION	
IV.A :	Two-Stage Transonic Axial-Flow Fan	33
IV.B :	Five-Stage Transonic Axial-Flow Compressor	36
IV.C :	Two-Stage Subsonic Axial-Flow Turbine	37
CHAPTER V :	CONCLUSIONS	40
SUGGESTIONS FOR FURTHER WORK		41
REFERENCES		42
APPENDIX A :	FLOW CHART OF COMPUTER PROGRAM	66
APPENDIX B :	FORTRAN PROGRAM LISTING	68

NOMENCLATURE

A	Defined in Eq. II-8
A_1, A_2, A_3	Constants used in estimation of deviation angles at off-design conditions
B	Defined in Eq. II-9
C	Defined in Eq. II-10
C	Absolute Velocity
C_p	Specific heat at constant pressure
D_{eq}	Equivalent diffusion factor
f	Fraction of mass flow through each streamtube
H	Stagnation enthalpy
h	Static enthalpy
M	Number of calculating stations
M	Meridional Mach number
M_{abs}	Absolute Mach Number
M_{rel}	Relative Mach number
N	Number of streamlines
n	Polytropic coefficient
p	Static pressure
q	Any flow quantity defined in Eq. II-7
r	Radius
s	Entropy
T	Stagnation temperature
t	Static temperature
U	Rotor velocity

W	Mass flow through the turbomachine
W	Relative velocity
x	Axial distance
α	Absolute fluid angle measured with respect to axial direction
β	Relative fluid angle measured with respect to axial direction
Δ	Defined in Eq. II-17
δ	Deviation angle
η	Stage efficiency
λ	Meridional streamline slope
λ'	Meridional streamline curvature
μ_1	Relaxation factory on axial velocity
μ_2	Relaxation factor on streamline shift
ω	Angular velocity of rotor
ρ	Density
γ	Ratio of specific heats
Σ	Defined in Eq. II-18

Subscripts :

o	Inlet or Stagnation conditions
c	Compressor
i	Denotes calculating station
in	Inlet to a blade row
j	Denotes streamline number
r	Component along radial direction
t	turbine

x	Component along axial direction
θ	Component along tangential direction

Superscripts :

'	Relative to rotor
*	Design or minimum loss values.

CHAPTER I

INTRODUCTION

I.A. GENERAL BACKGROUND

Before finalising the design of a turbomachine, a designer has to consider various annulus geometries and blade geometries. He has to consider design performance as well as performance at off-design conditions. Often a machine performing well at design condition may give quite unsatisfactory performance at off-design conditions. Hence theoretical methods of performance prediction of turbomachine become necessary and by employing such methods various designs can be studied for their performance at all operating conditions. A design can thus be finalised with some certainty before actual manufacture and testing with their problems of high cost and time delays.

Theoretical approach to the solution of aerodynamic problems in the design or performance prediction of fluid flow in axial turbomachines presents formidable problems. It involves the solution of the usual non-linear differential equations of fluid flow in most complicated geometries. An exact solution of the flow field, governed by the equations of three-dimensional unsteady, nonisentropic viscous flow through the complex of rotating and stationary blades and associated ducts is virtually impossible and hence calculation procedures must be approximate. Most effort has been concentrated on the formulation and solution of meaningful two-dimensional models of the flow field viz. 1) the hub-to-casing or meridional flow model - e.g. the S2 surface of Wu[1] and 2) the blade-to-blade or cascade

model e.g. the S1 surface of Wu[1]. The basis of each model is a judicious mixture of theoretical techniques, experimental correlations and experience. In the present investigation only study of hub-to-tip analysis or meridional flow model is undertaken. The fluid angles and fluid turning losses, which are necessary for the performance prediction of turbomachines are usually obtained from the cascade flow model. In the present case design fluid angles are fed in as input and the losses are accounted for by introduction of a polytropic exponent of expansion or compression depending on whether the machine is a turbine or a compressor.

In the earlier studies on turbomachines, the flow was assumed to be cylindrical and only velocity components in axial and tangential directions were considered. The radial component of velocity was neglected. This was quite reasonable with the earlier type of turbomachines where the blade height was usually small, the hub-tip ratio was high and the streamline were usually parallel to the axis. But with the advent of modern jet engine compressors and large steam and gas turbines, the hub-tip ratio has become low and the blade height is significant. Hence the flow tends towards conical rather than cylindrical and the radial component of velocity becomes significant. Streamline slope and curvature, therefore, play a dominant role in the flow field analysis. The shape of a streamline has a great effect on the radial pressure gradient and the radial distribution of other flow properties. The radial displacement of the fluid introduces curvature into the streamlines and this introduces additional radial pressure gradient, which is superimposed on the pressure gradient due to tangential motion. The changes in the radial pressure component can be

quite large in the case of long blades, i.e. the low pressure end of a turbomachine, even though the actual radial displacement of the streamline may be small. The magnitude of radial displacement of streamline increases considerably with the Mach number.

In order to take into account the effects of radial displacement of streamlines, the streamlines through the stage must be determined as accurately as possible for performance calculations. The slope of the streamlines allows one to determine the radial velocity component and the curvature enables the radial pressure gradient to be calculated. Thus, the slope and curvature of streamline becomes important in the performance calculation of low hub-tip ratio turbomachine and high Mach number flows.

In the past the methods that have been employed for calculating the flow field in axial turbomachines were usually based on relaxation techniques, streamline-curvature (S.C.) methods, actuator disk theories, simple radial equilibrium theories or matrix methods. Recently with the advent of fast digital computers and improved computational techniques, streamline curvature and matrix through flow methods have been favoured.

In the present investigation the streamline curvature method is used to predict the performance of an axial turbomachine when annulus geometry and blade geometry and a polytropic exponent to account for losses, and the turbomachine inlet conditions such as stagnation pressure and temperature, which are assumed to be constant radially, are given. The radially distributed temperature rise, pressure ratio and efficiency are subsequently determined as a function of mass flow and rotor speed.

In the S.C. method a curve is fitted through the points of intersection of stream surfaces with the radial lines and the properties of the curve, i.e. slope and curvature are taken to represent the streamline properties. These properties are used to calculate radial component of velocity and radial pressure gradient.

Before going into the details of the present study, a review of important work done previously is presented in the next section.

I.B. REVIEW OF PREVIOUS WORK:

Some of the earliest work done on the performance prediction of axial turbomachines was reported by Serovy and Anderson[2] and by Swan[3] whose work was based on the stream filament theory of Hol[illegible]nquist and Ramnie[4]. Both investigations were based on a finite-difference solution of the nonisentropic radial equilibrium and continuity equations at stations between blade rows. The steady, axisymmetric model of the flow used has been described thoroughly by later workers[4,5,6,7,8,9,10]. In each method, correlations of experimental data were developed and used for predicting the radial distribution of the fluid turning angle and of total-pressure loss for each blade row. Numerical solutions for single-stage geometries were presented, however, comparison with experimental results was not good, probably due to inadequate data correlations for flow angle and losses. Nevertheless, the[illegible] studies demonstrated the feasibility of numerical solution systems in generating both detailed flow passage distributions and overall compressor performance.

A similar approach in developing a program for computation of multistage axial-flow compressors was described by Jansen and Moffatt[11]. The steady, axisymmetric model was again used as formulated by Novak[12] and this formulation included improved schemes for iterative location of the axisymmetric stream surfaces and for computation of local values of stream surface slope and curvature.

Recently Crevelling and Carmody[13] also have developed an analysis program for multistage axial-flow compressors. The documentation of the computer program is incomplete. In reference 14 Daneshyar and Shalaan used a flow model similar to Novak[12] and their own data correlations to predict compressor performance. They discuss in somewhat more detail than in any earlier work, the numerical problems which are encountered in flow field solutions. They also examine the existence and uniqueness of the solutions obtained. This useful discussion is supplemented by papers of Marsh[15] and Wilkinson[16] who give a good deal of insight into some of these numerical difficulties. More recently, Mazumdar[17] describes a program developed by Davis[18] and compares it with others work. This program is primarily based on the flow model of Novak[12] combined with correlations available from earlier studies.

All of the preceding work is concerned with analysis for axial-flow-compressor geometries. These methods all assume a steady, axisymmetric flow. All calculations are at stations located in the axial spaces between blade rows. The basic flow model is, therefore, that identified as the blade-element model and described in reference 10.

Twisted turbomachine blades are usually evolved by a radial stacking of a series of blade sections or blade elements which are treated locally as 2-D sections to form complete blade. The blade-element model, hence, proposes that the blade-row characteristics can be determined if the performance of each blade element is known and that overall machine performance can then be obtained by an integration of the performance of each blade row. Fundamental differences in strategy exist between the above methods in the numerical solution techniques applied, including the means for estimating local values of stream surface position, slope and curvature.

A somewhat different means for formulation of the performance prediction problem for axial flow turbomachines has been proposed and used by Marsh[19]. This method derives a Poisson type equation for the streamfunction. Also calculating planes are taken inside blade rows, by assuming the shape of mean stream surface in the blade row. Frost[20] combines this method - the matrix through-flow method - with the S.C. method. More recently, Marsh and Bosman[21] have improved the matrix-through flow method to predict performance of various types of turbomachines. This method includes an improved loss model based on Horlock's work[22]. The matrix through flow method does not avoid the requirement for input of key empirical data correlations and in example solutions currently available, does not appear to offer a clear improvement in any area of performance calculation except a little saving in computing time. Its disadvantage over the S.C. method is that it requires more computer core storage.

Additional examples of related research on turbomachine performance prediction are contained in references 23 to 25. A procedure and computer program for axial-flow turbine analysis is described by Flagg[23]. Another is discussed by Renaudin and Somm[24]. A novel method for avoiding solution convergence problems is used by them, which should be applicable to other turbomachine cases. Ribaut[25] has outlined a system for a very general analysis of the through-flow field, but unfortunately, the problems in application appear to be substantial.

In the present investigation the flow model is based on the formulation developed by Moorthy[7]. This formulation gives a better physical picture of the flow and is suitable for rapid digital computation. The meridional Mach Number and the streamline slope and curvature terms appear explicitly in the radial equilibrium equation, so as to provide a better physical appreciation of the effects of these factors. Moreover, when this formulation is reduced to the two-dimensional case, the dynamic equation of fluid flow reduces to the well-known expression for the change in Prandtl-Meyer angle across a Mach line. This method was employed by Moorthy[7] to study the performance prediction of a turbine stage using a high speed digital computer and the results of study were said to be in very good agreement with experimental values.

In the next chapters, this method is developed for multistage axial turbomachines and development of digital computer line up for rapid calculation of performance prediction of multi-stage turbomachine is presented.

CHAPTER II

FORMULATION OF THE PROBLEM

II.A. PRELIMINARY CONSIDERATIONS:

In this chapter the performance calculation method for multistage turbomachines is developed following Moorthy[7]. The schematic diagram of meridional flow model is given in Figure 1. The flow is analysed at a station immediately downstream of a blade row by considering the known upstream conditions, the annulus configuration and the blade shape. This method can be used for both the direct problem, i.e. performance prediction of given turbomachine and the inverse problem i.e. determination of cascade characteristics, given other flow properties. The present investigation is limited to the direct case.

Steady, axisymmetric compressible flow is assumed. The calculating planes are located in the axial spaces between blade rows. Calculations are performed at various radial points at each plane, the radial points being selected so that an equal fraction of total mass flow passes through each stream tube. From the simultaneous solution of the radial equilibrium and continuity equations, axial velocities and streamline radii are determined. The effect of streamline slope and curvature is considered in calculating these quantities. Once axial velocity and streamline radii are determined, other flow properties are easily determined. The losses due to real fluid effects such as viscosity and shocks are accounted for by the specification of a polytropic ~~efficiency~~ coefficie

II.B. ASSUMPTIONS:

Since the flow in turbomachines is quite complex, some reasonable assumptions must be made, so that a mathematical representation of the flow field is tenable. Hence in addition to the previous assumption of steady, axisymmetric flow and accounting of losses by introduction of polytropic coefficient, the following assumptions are made.

1. There is no heat exchange between adjacent stream surfaces. Although the temperature difference between root and tip can be quite large in a practical machine with long blades, it can be said, that when the fluid velocity is large, the adjacent fluid particles do not have sufficient time for any appreciable heat exchange. Further, in the blade-element method, the adjacent stream surfaces are assumed to be separated by short radial distances, the actual temperature difference between them is small. Therefore, one may be justified in neglecting heat exchange.

2. The total or stagnation values of enthalpy, density and angular momentum per unit mass of fluid are constant on a streamline outside any blade row. This does not mean that their values do not change across a blade row, i.e. in the passage of the fluid through a row. This assumption means that the gradients of the above properties are subsequently zero along the streamlines.

3. The boundary layer effect is accounted for by the inclusion of boundary layer blockage factors, which give the percentage of the annulus area not blocked by boundary layers at the hub and the tip.

4. Interference effects between adjacent blade rows are neglected. The flow downstream of each blade row is assumed to be mixed completely before

entering the next blade row.

5. Tip leakage effects and secondary flow effects are neglected except as included in the specification of polytropic coefficient. The effects of sweep and dihedral of blades are neglected.

6. The specific heat at constant pressure is assumed constant.

7. Shock losses in transonic compressors are assumed to be negligible.

II.C. DERIVATION OF RADIAL EQUILIBRIUM EQUATION :

In this section, details of the derivation of the radial equilibrium equation are given briefly. This derivation mainly follows Moorthy's[7] formulation.

The governing equations for steady inviscid axisymmetric compressible flow in the absence of body forces and heat transfer can be written as follows :

Continuity Equation :-

$$\frac{1}{r}\frac{\partial}{\partial r}(\rho r C_r) + \frac{\partial}{\partial x}(\rho C_x) = 0 \qquad \text{(II.1)}$$

Equation of Motion in Radial Direction :-

$$C_x \frac{\partial C_r}{\partial x} + C_r \frac{\partial C_r}{\partial r} - \frac{C_\theta^2}{r} = -\frac{1}{\rho}\frac{\partial p}{\partial r} \qquad \text{(II.2)}$$

Equation of Motion in Axial Direction :-

$$C_x \frac{\partial C_x}{\partial x} + C_r \frac{\partial C_x}{\partial r} = -\frac{1}{\rho}\frac{\partial p}{\partial x} \qquad \text{(II.3)}$$

Energy Equation :-

$$h + \frac{1}{2}(C_x^2 + C_r^2 + C_\theta^2) = H \qquad (II.4)$$

where C_r, C_θ, C_x are the velocity components, h is the static enthalpy and eq. (II.4) defines H, the stagnation enthalpy.

Combined first and second laws of thermodynamics give

$$t\frac{\partial s}{\partial r} - \frac{\partial h}{\partial r} = -\frac{1}{\rho}\frac{\partial p}{\partial r} \qquad (II.5)$$

$$t\frac{\partial s}{\partial x} - \frac{\partial h}{\partial x} = -\frac{1}{\rho}\frac{\partial p}{\partial x} \qquad (II.6)$$

where s is the entropy and t, ρ and p are static values of temperature, density and pressure respectively.

The above equations are now expressed in terms of total derivatives along meridional streamlines. These streamlines are the intersection lines of axisymmetric stream surfaces with the meridional plane containing the r and x directions. Henceforth streamlines will refer to meridional streamlines.

Along a streamline, the radius r is an implicit function of x. The total derivative of any flow quantity q along the meridional streamline with reference to x for steady axisymmetric flow is given by,

$$\frac{dq}{dx} = \frac{\partial q}{\partial x} + \frac{dr}{dx}\frac{\partial q}{\partial r} \qquad (II.7)$$

$$= \frac{\partial q}{\partial x} + \frac{\partial q}{\partial r} \qquad (II.8)$$

or $$\frac{d}{dx} \equiv \frac{\partial}{\partial x} + \lambda \frac{\partial}{\partial r} \qquad (II.9)$$

where $$\lambda = \frac{dr}{dx} = \frac{dr}{dt} / \frac{dx}{dt} = \frac{C_r}{C_x} \qquad (II.10)$$

is the streamline slope at the point considered.

Using equation (II.9) in equations of motion (II.2 and II.3) and combining them after multiplying by C_r and C_x respectively, we get after some rearrangement,

$$(1+\lambda^2) C_x \frac{dC_x}{dx} + \lambda\left(C_x^2\lambda' - \frac{C_\theta^2}{r}\right) + a^2 \frac{d}{dx}(\log \rho) = 0 \qquad (II.11)$$

where 'a' is the speed of sound and $\lambda' = \frac{d^2 r}{dx^2}$ is the streamline curvature. The equation of continuity is modified using equations (II.9) and (II.10) to

$$C_x \frac{d}{dx}(\log \rho) = -\left[\frac{dC_x}{dx} + C_x\left(\frac{\partial \lambda}{\partial r} + \frac{\lambda}{r}\right)\right] \qquad (II.12)$$

Eliminating $\frac{d}{dx}(\log \rho)$ from equations (II.11 and II.12) and using the Meridional Mach number

$$M = \sqrt{\frac{(1+\lambda^2) C_x^2}{a^2}} \qquad (II.13)$$

equation (II.14) is obtained.

Hence

$$\frac{dC_x}{dx} = -\frac{C_x}{1-M^2}\left[\frac{\lambda M^2}{1+\lambda^2}\left(\frac{C_\theta^2}{rC_x^2} - \lambda'\right) + \frac{\partial \lambda}{\partial r} + \frac{\lambda}{r}\right] \qquad (II.14)$$

As evident from (II.14), for negligible Mach Numbers the circumferencial velocity and streamline curvature in the meridional plane have no effect on axial velocity changes. If λ and M are both not small, the circumferential velocity and the streamlines curvature becomes important as in the case of high subsonic, transonic, supersonic turbomachines with tapered annuli.

Thus equation (II.14) gives a better physical appreciation of effect of Mach number, streamline slope and curvature and also indicates that for a singular solution to exist the meridional Mach number, not the relative Mach number is important.

Now this equation is used in the radial equation of motion (II.2) along with (II.10) to obtain the radial pressure gradient in a turbomachine, i.e. the radial equilibrium equation.

Using equation (II.10)

$$\frac{dC_r}{dx} = \frac{d}{dx}(\lambda C_x) = \lambda \frac{dC_x}{dx} + \lambda' C_x \qquad (II.15)$$

Using this equation in Equation (II.2) and substituting for $\frac{dC_x}{dx}$ from Equation (II.14) we obtain

$$-\frac{1}{\rho}\frac{\partial p}{\partial r} = \frac{-\lambda C_x^2}{1-M^2}\left\{\frac{\lambda M^2}{1+\lambda^2}\left(\frac{C_\theta^2}{r C_x^2} - \lambda'\right) + \frac{\partial \lambda}{\partial} + \frac{\lambda}{r}\right\}$$

$$+ \lambda' C_x^2 - \frac{C_\theta^2}{r} \qquad (II.16)$$

Defining $$\Delta = \frac{\lambda^2}{1-M^2} \qquad (II.17)$$

and $$\sum = \frac{\lambda^2 M^2}{(1+\lambda^2)(1-M^2)} = \frac{\Delta M^2}{(1+\lambda^2)} \qquad (II.18)$$

Equation (II.16) is transformed to

$$-\frac{1}{\rho}\frac{\partial p}{\partial r} + \frac{\Delta C_x^2}{r} + \frac{1}{2(1-M^2)}\frac{\partial \lambda^2}{\partial r} + (1+\Sigma)\left(\frac{C_\theta^2}{r} - \lambda' C_x^2\right) = 0 \qquad (II.19)$$

This is the generalised radial equilibrium equation of turbomachines. For turbomachines of cylindrical annuli equation (II.19) becomes simply $\frac{1}{\rho}\frac{dp}{dr} = \frac{C_\theta^2}{r}$. This equation implies that radial velocity C_r is zero at inlet and exit from a blade row. For the present investigation neither λ nor M is negligible, hence Δ or Σ are not negligible.

So far no statement regarding entropy generation has been made. In general losses result in a non-uniform entropy. However it is possible to postulate that the polytropic equation P/ρ^n = constant holds. Using this relation, equation (II.5) can be written as

$$\frac{\partial h}{\partial r} = \frac{\gamma}{\gamma-1}\frac{n-1}{n}\frac{1}{\rho}\frac{\partial p}{\partial r} \qquad (II.20)$$

Now for a compressor $\frac{\gamma}{\gamma-1}\frac{n-1}{n} = \frac{1}{\eta_c}$

and for a turbine $\frac{\gamma}{\gamma-1}\frac{n-1}{n} = \eta_t$

where η_c and η_t are the respective stage efficiencies here assumed constant for all stages and for all streamlines.

Hence

$$\frac{\partial h}{\partial r} = \eta_t \frac{1}{\rho}\frac{\partial p}{\partial r} \text{ (turbine)}$$

$$\frac{\partial h}{\partial r} = 1/\eta_c \frac{1}{\rho}\frac{\partial p}{\partial r} \text{ (compressor)}$$

Expressing h in terms of H and velocity component the r.e.e. for compressors and turbines becomes respectively

$$-\eta_c \frac{\partial H}{\partial r} + \frac{\eta_c}{2}(1+\lambda^2)\frac{\partial}{\partial r}(C_x^2) + \frac{1}{2}\{\eta_c + \frac{1}{1-M^2}\} C_x^2 \frac{\partial \lambda^2}{\partial r}$$

$$+ \frac{\eta_c}{2}\frac{\partial C_\theta^2}{\partial r} + (1+\Sigma)(\frac{C_\theta^2}{r} - \lambda' C_x^2) + \frac{\Delta C_x^2}{r} = 0 \qquad \text{(II.21)}$$

$$-\frac{1}{\eta_t}\frac{\partial H}{\partial r} + \frac{1}{2}\frac{1+\lambda^2}{\eta_t}\frac{\partial}{\partial r} C_x^2 + \frac{1}{2}\{\frac{1}{\eta_t} + \frac{1}{1-M^2}\} C_x^2 \frac{\partial \lambda^2}{\partial r}$$

$$+ \frac{1}{2\eta_t}\frac{\partial C_\theta^2}{\partial r} + (1+\Sigma)(\frac{C^2}{r} - \lambda' C_x^2) + \frac{\Delta C_x^2}{r} = 0 \qquad \text{(II.22)}$$

II.D. Auxiliary Equations :-

In addition to the r.e.e. and continuity equation a number of auxiliary equations are necessary to calculate flow

in turbomachines. The continuity equation in the following integral form is suitable for the streamline curvature method.

$$W = 2\pi \int_{r_{i,1}(r_{hub})}^{r_{i,N}(r_{tip})} \rho C_x \, r \, dr \qquad (II.23)$$

or between two adjacent streamlines the mass flow becomes

$$fW = 2\pi \int_{r_{i,j-1}}^{r_{i,j}} \rho C_x \, r \, dr \qquad (II.24)$$

where f is a fraction of mass flow between streamlines (j-1) and j, the index i refers to the calculating plane, each of which is divided into (N-1) stream tubes which are labelled by the index of j.

The enthalpy rise across a blade row can be found from Euler's equation

$$\Delta H = (\omega r C_\theta)_{i,j} - (\omega r C_\theta)_{i-1,j} \text{ along streamline } j \qquad (II.25)$$

or
$$H_{i,j} = H_{i-1,j} + (\omega r C_\theta)_{i,j} - (\omega r C_\theta)_{i-1,j} \qquad (II.26)$$

Hence temperature rise for a perfect gas is

$$\Delta T = \frac{(\omega r C_\theta)_{i,j} - (\omega r C_\theta)_{i-1,j}}{C_p} \qquad (II.27)$$

$$\text{or} \qquad T_{i,j} = T^{\circ}_{i-1,j} + \frac{(\omega r\, C_\theta)_{i,j} - (\omega r\, C_\theta)_{i-1,j}}{C_p} \qquad \text{(II.28)}$$

The absolute circumferential-velocity is given by

$$C = C_\theta \tan \alpha \qquad \text{(II.29)}$$

and relative fluid angle is given by

$$\beta = \tan^{-1}\left(\frac{W_\theta}{C_x}\right) = (C_\theta - \omega r)/C_x \qquad \text{(II.30)}$$

The density distribution is determined from the polytropic equation. It can be shown that

$$\rho_{i,j} = \rho^{\circ}_{i-1,j} \left[\frac{H_{i,j} - \frac{1}{2}\left(C^2_{x\,i,j} + C^2_{\theta i,j} + C^2_{r\,i,j}\right)}{H_{i-1,j}}\right]^{\frac{1}{n-1}} \qquad \text{(II.31)}$$

All the above equations are valid for any calculating plane. However the angular velocity ω is non-zero only for a rotor, i.e. ΔH in II.25 is non-zero only if the plane 'i' follows a rotor. Appropriate modifications must also be made in the other equations.

The radial equilibrium equation and continuity equation along with the auxiliary equation are solved numerically in the inter blade row gap to obtain the axial velocity and streamline radius. The method is described in detail in the next chapter.

II.E. ESTIMATION OF FLUID ANGLES AT OFF-DESIGN CONDITIONS:-

In the present investigation, absolute fluid angles at the trailing edge station of blade rows at design point only are specified. Hence a procedure is necessary to estimate fluid angles at other operating conditions. Swan's[3] method of correlation of the deviation angle δ with respect to equivalent diffusion factor D_{eq} is chosen.

Fig. 3 shows the trend in $\delta-\delta^*$ versus $D_{eq} - D_{eq}^*$ which was found from an examination of Double Circular Arc (D.C.A.) rotor blade elements. The data were grouped in relative Mach number ranges to show the effect of this parameter. No noticeable effect of spanwise location occurred. In general, the variation is represented by the following equation.

$$\delta-\delta^* = [A_1 - A_2 (M'_{in} - 0.60)](D_{eq} - D_{eq}^*) \qquad (II.32)$$

where starred quantities represent design values, and $A_1 = 6.40$ and $A_2 = 9.45$ for D.C.A. rotor blade elements.

The constant 0.6 was used because data obtained at relative Mach numbers below 0.6 did not indicate any Mach number influence. Similar correlations were obtained from limited stator data. No Mach number effect was applied, because of a lack of data on stators in high Mach number range. Thus

$$\delta-\delta^* = A_3 (D_{eq} - D_{eq}^*) \qquad (II.33)$$

where A_3 = 2.4 for D.C.A. stator blade elements.

Once δ is determined, fluid angle at the exit plane of a blade row is determined as follows.

$$\beta = \beta^* - (\delta - \delta^*) \qquad \text{(II.34)}$$

Due to lack of data, for other blade types, the off-design fluid angles are assumed to be the same as those at design condition.

CHAPTER III

METHOD OF SOLUTION

III.A. FINITE DIFFERENCE EQUATIONS:-

In order to solve the radial equilibrium equation (II.19), and the continuity equation (II.23), a finite-difference method is used. The finite-difference grid in the meridional plane is shown in Fig.1.

The first-order derivatives with respect to streamline radius, 'r', like $\frac{\partial C_x^2}{\partial r}$, $\frac{\partial \lambda^2}{\partial r}$, $\frac{\partial H}{\partial r}$ etc., which appear in the radial equilibrium equation, are approximated by the backward difference. That is, at grid point (i,j),

$$\left(\frac{\partial H}{\partial r}\right)_{i,j} = (H_{i,j} - H_{i,j-1}) / (r_{i,j} - r_{i,j-1}) \qquad \text{(III.1)}$$

With the help of the above equation the radial equilibrium equation, while integrated in radial direction, for a compressor is transformed into the following finite-difference equation.

$$-\eta_c (H_{i,j} - H_{i,j-1}) + \frac{\eta_c}{4} (2 + \lambda^2_{i,j} + \lambda^2_{i,j-1}) (C^2_{x_{i,j}} - C^2_{x_{i,j-1}})$$

$$+ \frac{1}{4} \left[\left(\eta_c + \frac{1}{1-M^2_{i,j}}\right) C^2_{x_{i,j}} + \left(\eta_c + \frac{1}{1-M^2_{i,j-1}}\right) C^2_{x_{i,j-1}}\right] (\lambda^2_{i,j} - \lambda^2_{i,j-1})$$

$$+ \frac{\eta_c}{2}\left(C^2_{\theta_{i,j}} - C^2_{\theta_{i,j-1}}\right) + \frac{\left(r_{i,j} - r^2_{i,j-1}\right)}{2}\left[\frac{\Delta_{i,j}}{r_{i,j}} C_{x_{i,j}}\right.$$

$$+ \frac{\Delta_{i,j-1}}{r_{i,j-1}} C^2_{x_{i,j-1}} + \left(1+\Sigma_{i,j}\right)\left(\frac{C^2_{\theta_{i,j}}}{r_{i,j}} - \lambda'_{i,j} C^2_{x_{i,j}}\right)$$

$$\left. + \left(1+\Sigma_{i,j-1}\right)\left(\frac{C^2_{\theta_{i,j-1}}}{r_{i,j-1}} - \lambda'_{i,j-1} C^2_{x_{i,j-1}}\right)\right] = 0 \qquad \text{(III.2)}$$

For a turbine η_c is replaced by $1/\eta_t$.

The equations (II.25, II.29 and II.30) in the finite-difference scheme are as follows:

$$H_{i,j} = H_{i-1,j} + \omega\left(r_{i,j} C_{\theta_{i,j}} - r_{i-1,j} C_{\theta_{i-1,j}}\right) \qquad \text{(III.3)}$$

$$C_{\theta_{i,j}} = C_{x_{i,j}} \tan \alpha_{i,j} \qquad \text{(III.4)}$$

Hence equation (III.3) becomes

$$H_{i,j} = H_{i-1,j} + \omega\left(r_{i,j} C_{x_{i,j}} \tan \alpha_{i,j} - r_{i-1,j} C_{\theta_{i-1,j}}\right) \qquad \text{(III.5)}$$

$$\tan \beta_{i,j} = \left(C_{\theta_{i,j}} - \omega r_{i,j}\right) / C_{x_{i,j}} \qquad \text{(III.6)}$$

Using equations (III.4) and (III.5) in equation (III.2), the following quadratic equation in $C_{x_{i,j}}$ is obtained.

$$A\ C_{x_{i,j}} + B\ C_{x_{i,j}} + C = 0 \qquad \text{(III.7)}$$

where $A = \frac{\eta_c}{4}\left(2 + \lambda^2_{i,j} + \lambda^2_{i,j-1}\right) + \frac{1}{4}\left(\eta_c + \frac{1}{1-M^2_{i,j}}\right)\left(\lambda^2_{i,j} - \lambda^2_{i,j-1}\right)$

$$+ \frac{\eta_c}{2}\tan^2\alpha_{i,j} + \frac{\left(r_{i,j} - r_{i,j-1}\right)}{2}\left[\frac{\Delta_{i,j}}{r_{i,j}} + \left(1 + \Sigma_{i,j}\right)\right.$$

$$\left.\left(\frac{\tan^2\alpha_{i,j}}{r_{i,j}} - \lambda'_{i,j}\right)\right] \qquad \text{(III.8)}$$

$$B = -\ \eta_c\ \omega\, r_{i,j} \tan\alpha_{i,j} \qquad \text{(III.9)}$$

and $C = -\ \eta_c\ \left(H_{i-1,j} - \omega r_{i-1,j}\ C_{\theta\ i-1,j} - H_{i,j-1}\right)$

$$+ C^2_{x_{i,j-1}}\left[\frac{1}{4}\left\{\left(\eta_c + \frac{1}{1-M^2_{i,j-1}}\right)\left(\lambda^2_{i,j} - \lambda^2_{i,j-1}\right) - \left(2 + \lambda^2_{i,j} + \lambda^2_{i,j-1}\right.\right.\right.$$

$$\left.\left.\left. + \frac{\left(r_{i,j} - r_{i,j-1}\right)}{2}\left\{\frac{\Delta_{i,j-1}}{r_{i,j-1}} - \left(1 + \Sigma_{i,j-1}\right)\lambda'_{i,j-1}\right\}\right]\right.$$

$$+ \frac{1}{2}\ C^2_{\theta\ i,j-1}\left[\frac{\left(r_{i,j} - r_{i,j-1}\right)}{r_{i,j-1}}\left(1 + \Sigma_{i,j-1}\right) - 1\right] \qquad \text{(III.10)}$$

The continuity equation in the integral form is expressed in the following finite-difference form.

$$f\ W = \frac{\pi}{2}\left[\rho_{i,j}\ C_{x_{i,j}} + \rho_{i,j-1}\ C_{x_{i,j-1}}\right]\left(r^2_{i,j} - r^2_{i,j-1}\right)$$

(III.11)

The numerical solution of the finite-difference equations (III.7) and (III.11) with the help of equations (III.4) to (III.6) is described in the next section.

III.B. SOLUTION OF FINITE-DIFFERENCE EQUATIONS:-

The calculating grid in the meridional plane is shown in Fig.1. Calculating stations are taken after rotor and stator blade rows. For calculating stations after rotor blade rows ω is the angular speed of the rotor and for calculating stations after stator blade rows ω is zero. The exit flow at each blade row is taken as the inlet flow to the succeeding blade row. The calculation proceeds in the following steps.

1. At each station the annulus is first divided into a number of streamtubes of equal area. In this case 1/f/are number of streamtubes, where 'f' is the fraction of mass flow passing through each streamtube. The streamlines, thus generated serve as temporary guides in the iteration process and are replaced by newly calculated streamlines after each overall iteration.

2. The first three calculating stations are taken outside the first blade row. The flow field at two stations is calculated assuming one-dimensional flow. The slope and curvature of streamlines of these two stations are assumed to be zero. From third station onwards the calculation proceeds as follows.

3. The properties of streamlines i.e. slope and curvature at all grid points are computed by fitting a three-point parabola.

4. For the first overall iteration, the axial velocity at each grid point is assumed to be equal to the axial velocity at the first two stations.

5. At each grid point, the terms such as M, Δ, Σ, C_θ, H, ρ and tan β are calculated from assumed $C_{x_{i,j}}$ and given values of tan α.

6. The radial equilibrium equation is now integrated from streamline (j-1) to streamline j. A new value of $C_{x_{i,j}}$ is obtained by solving the quadratic equation (III.7).

7. The new value of $C_{x_{i,j}}$ is checked for convergence. If it is not converged to a specified tolerance, steps 5 and 6 are repeated using the following value of axial velocity.

$$C^{k}_{x_{i,j}} = C^{k-1}_{x_{i,j}} + \mu_1 \left(C^{k}_{x_{i,j}} - C^{k}_{x_{i,j-1}} \right) \qquad \text{(III.12)}$$

(weighted)

where μ_1 is the relaxation factor on axial velocity. This relaxation factor is necessary to avoid divergence of axial velocity calculations. The value of μ_1 is found by trial and error. For the present case μ_1 is taken as 0.1.

8. After axial velocity is calculated at each grid point in a particular calculating station, new values of streamline radii at that particular station are calculated from the continuity equation (III, 11).

9. The tip radius, thus calculated, should coincide with the given tip radius, at that particular station. But, usually, a tip radius, which is either small or large compared with the given tip radius is calculated. A new value of hub axial velocity is calculated as follows and used in the next iteration to calculate tip radius.

For the second iteration, the hub axial velocity is taken as 0.9 times of the hub axial velocity of first iteration. From third iteration onwards, the hub axial velocity is determined by linear interpolation of hub axial velocities of the previous two iterations. Thus, for third iteration, the hub axial velocity is given by intersection of P_1 P_2 and AB and for n^{th} iteration, it is given by intersection of P_{n-2} P_{n-1} and AB, as shown Fig. 2.

10. Steps 5 to 9 are repeated with the new hub axial velocity until the calculated tip radius agrees with the given tip radius within specified limit.

11. In this way, the solution marches down upto (M-2) th calculating station, which is the first station outside the

last blade row. Here M is the total number of calculating stations. At the last two stations, the flow properties are assumed to be the same as those of the $(M-2)^{th}$ station.

12. For the next overall iteration, new streamline radii are obtained by adding a weighted fraction of the shift in radius, to the radii of the previous overall iteration. That is,

$$r^{k}_{i,j\ (weighted)} = r^{k-1}_{i,j} + \mu_2 \left(r^{k}_{i,j} - r^{k}_{i,j-1}\right)$$

where μ_2 is the relaxation factor on streamline radial shift. Wilkinson[15] derives explicit expressions for the optimum relaxation factor as function of grid aspect ratio, Mach number and the method for finding slopes and curvature of the meridional streamlines for a simple two-dimensional flow. For the present study of axisymmetric flow, explicit expression for relaxation factor is not derived. It is taken to be 0.1 as suggested in reference 17.

13. Using the weighted streamline radii, the calculation from steps 3 to 12 is repeated.

14. In successive overall iterations, the calculated streamline radii converge within a specified tolerance. Usually 10 to 15 overall iterations are needed for convergency on streamline radii.

15. After calculating the velocities and other flow properties at each grid point, the mass averaged performance after each stage is calculated using the procedure of reference 9.

The mass-averaged temperature rise across a blade row is given by the following equation,

$$\left(\frac{T_i}{T_o}\right)_{m,a} - 1.0 = \frac{2\pi K_e}{W} \int_{r_{i,hub}}^{r_{i,tip}} \left(\frac{T_i}{T_o}\right) \rho C_x \, d_r^2 \qquad \text{(III, 13)}$$

where T_o is the inlet stagnation temperature and K_e is temperature-rise or energy exchange factor. This factor is necessary, in addition to the boundary layer blockage factor K_b, to account for the wall boundary layer effect on temperature-rise.

Similarly, a correction factor K_p for the mass-averaged pressure ratio is applied and the mass-averaged pressure ratio is given by the following equation:

$$\left(\frac{P_i}{P_o}\right)_{m,a} = \frac{2\pi K_p}{W} \left\{ \int_{r_{i,hub}}^{r_{i,tip}} \left[\left(\frac{P_i}{P_o}\right)^{\frac{\gamma-1}{\gamma}} - 1\right] \rho C_x \, dr^2 \right\} + 1 \qquad \text{(III, 14)}$$

where P_o is the inlet stagnation pressure.

From survey of limited experimental data, the values of K_p and K_e are taken to be 1, in reference 10

After mass-averaged pressure ratio and temperature rise, the adiabatic efficiency and polytropic efficiency are determined stage-by-stage.

$$\text{Adiabatic Efficiency } \eta_{ad} = \frac{(P_i/P_o)_{m.a}^{\frac{\gamma-1}{\gamma}} - 1}{(T_i/T_o)_{m.a} - 1} \qquad \text{(III.15)}$$

$$\text{Polytropic Efficiency } \eta_p = \left(\frac{\gamma-1}{\gamma}\right) \frac{\ln (P_i/P_o)_{m.a}}{\ln (T_i/T_o)_{m.a}} \qquad \text{(III.16)}$$

In the following section details of numerical difficulties encountered in calculation of velocities and streamline properties and their elimination procedures are described.

II.C. NUMERICAL DIFFICULTIES AND THEIR ELIMINATION :

The accuracy of any streamline curvature method depends on the accuracy of estimating streamline properties, i.e., slope and curvature of meridional streamlines. Since, during successive iterations, the streamline may not be smooth, a suitable method of curve fitting should be employed. Especially the curvature is very sensitive to the smoothness of the streamline. In the present study, the spline method described in reference 29 is first employed to find streamline slope and curvature. Even though calculated slope is reasonably accurate, curvature calculated by this method is usually very high, especially when

the streamline is not smooth. This high value of curvature gives difficulties in calculating axial velocity. Afterwards a second degree polynominal passing through three successive points is employed. This method gives fairly accurate values of slope and curvature, even when the streamline is not smooth.

Daneshyar and Shalaan[14] had shown that under certain conditions the truncation errors in the numerical solution can become large and hence give rise to the violation of uniqueness conditions. The numerical method may then give wrong answers to the physical problem. The conditions for existence and uniqueness may be violated when axial velocities are small (e.g. near stall) or when there are regions of choked flow. In this case the program may give large value of tip radius. Hence in adjusting tip radius, small velocities may occur at some streamlines. This may further give rise to negative velocities. Since negative velocities give difficulties in calculating other flow parameters, these velocities are replaced by some reasonable positive values.

In determining axial velocity from radial equilibrium equation by the quadratic equation (III.7), the discriminant (i.e. B^2-4AC) may become negative. Hence solution of r.e.e. fails. From expression for A (III.8), it is seen that A is always positive. Hence $\acute{G}$ should be small or negative, so that the discriminant is positive. The value of $\acute{G}$ mainly depends upon

absolute circumferential velocity. Hence the discriminant becomes negative when either C_x or α is large. So the value of C_x is limited to a maximum value. This further eliminates very high Mach numbers. High Mach numbers may give rise to numerical instability because the term $1/(1-M^2)$, appears in r.e.e. Even when C_x is limited, the discriminant may become negative. In such cases, the discriminant is made equal to zero for small negative values. For high negative values of discriminant, the program terminates present data and proceeds on to next data.

CHAPTER IV

RESULTS AND DISCUSSION

The method described in previous chapters is used to predict the performance of the following turbomachines.

1. Two-stage Transonic Axial-Flow Fan[26]
2. Five-stage Transonic Axial-Flow Compressor[27]
3. Two-stage Subsonic Axial-Flow Turbine[28].

Before going into details of results and discussion, theoretical variation of performance parameters with axial or meridional velocity is described.

Meridional velocity $C_m = C_x \sqrt{1+ \lambda^2}$ IV.1

is approximately equal to C_x for small values of

Absolute Mach number is given by

$$M_{abs} = \frac{C_x}{a} \sqrt{(1 + \lambda^2 + \tan^2 \alpha)} \qquad \text{IV.2}$$

and speed of sound

$$a = \sqrt{\gamma R t} = \sqrt{(\gamma-1)h} = \sqrt{(\gamma-1)\left[H - \frac{1}{2} C_x^2 (1 + \lambda^2 + \tan^2 \alpha)\right]} \qquad \text{IV.3}$$

Since C_x^2 is always smaller than H, 'a' is approximately constant for small changes in C_x, and α at design point is same as that in experiments. Hence radial variation of M_{abs} essentially follows that of C_x or C_m.

Relative Mach number is given by

$$M_{rel} = \frac{C_x}{a} \sqrt{(1 + \lambda^2 + \tan^2 \alpha - \frac{2\omega r \tan \alpha}{C_x} + \frac{\omega^2 r^2}{C_x^2})} \qquad \text{IV.4}$$

If the wheel speed ωr is of higher order than C_x, then discrepances between experimental and theoretical values of M_{rel} will be small otherwise, the radial variation of M_{rel} follows that of C_x.

Relative fluid angle for a rotor is given by

$$\beta = \tan^{-1} (\tan \alpha - \frac{\omega r}{C_x}) \qquad \text{IV.5}$$

Hence β decreases as C_x increases and converse is true.

Total temperature ratio across a rotor blade row 'i' and along streamline 'j' is given by

$$\frac{T_{i,j}}{T_{i-1,j}} = \frac{H_{i,j}}{H_{i-1,j}} = \frac{H_{i-1,j} + \omega [(rC_\theta)_{i,j} - (rC_\theta)_{i-1,j}]}{H_{i-1,j}} \qquad \text{IV.6}$$

Since $r_{i,j}$ and $r_{i-1,j}$ are approximately equal,

$$\frac{T_{i,j}}{T_{i-1,j}} = 1 + \frac{\omega r_{i,j}}{H_{i-1,j}} [(C_x \tan \alpha)_{i,j} - (C_x \tan \alpha)_{i-1,j}] \qquad \text{IV.7}$$

Hence total temperature ratio is dependent on three parameters, axial velocity at leading and trailing edges of rotor and leading edge stagnation enthalpy. The total pressure ratio variation essentially follows that of the total temperature ratio.

In the following sections, overall performance and radial variation of performance parameters are presented for the three examples. Also consistency in the predicted and experimental variation of various parameters is examined and wherever possible, explanations are offered.

IV A. Two-Stage Transonic Axial-Flow Fan (Reference 26):-

This fan was designed for a tip speed of 1450 ft/sec, an overall pressure ratio of 2.8 and a corrected mass flow of 184.2 lb/sec. The fan was designed without inlet guide vanes and air enters the first rotor axially. The inlet hub-to-top ratio was 0.4. and exit hub-to-top ratio was 0.68. Rotor and stator blade sections for both stages of the fan are multiple-circular-arc (MCA) airfoils designed on conical surfaces which approximate stream surfaces of revolution.

The computing time taken on IBM 370/165 computer for the execution of entire performance map is about 2.5 minutes. For a typical point near design condition, the computing time is 10 to 12 seconds.

IV.A.1 Overall Performance :- The overall performance data for the two-stage fan are presented in figure 4. These data cover a range of corrected speeds from 50 to 100 percent design. The pressure ratios predicted by this method are usually higher than the experimental values. The efficiences are in good agreement with the experimental

values, which is to be expected, since the actual value of polytropic efficiency at each point is fed in as input.

Adiabatic efficiency at design point is 81 percent, which is almost equal to the experimental value of 80.8 percent. Peak efficiency at design speed is 84.4 and occurred at a pressure ratio 3.29. Corresponding experimental values are 85 percent and 2.95 respectively. Peak efficiency increased from 82 percent at 50 percent design speed to 84.4 percent at design speed. Experimental peak efficiency at 50 percent design speed is 82.2 percent.

Overall performance of first stage is presented in Figure 5. Efficiency at design operating condition is 81.8 percent which is 3.6 percent less than the experimental value. Pressure ratios at design speed is in good agreement with experimental values. At other speeds the predicted values of pressure ratio are not in good agreement with the experimental values. The predicted efficiencies are more scattered than the experimental values for the first stage as compared to the whole two-stage fan. This may be due to the assumption of constant polytropic coefficient for all stages.

IV.A.2 Spanwise Variation of Pertinent Parameters at Design Point.

The predicted spanwise variation of pertinent parameters at design point for two-stage fan is presented and compared with experimental variation in figure 6.

The meridional velocity profile at L.E.of rotor 1 predicted by this method is higher than the experimental profile. Spanwise variation of M_{abs}, M_{rel} and β are consistent with C_m variation. No definite explanation is offered for the differences in C_m profiles, but it may be due to assumption of one-dimensional flow and zero slope and curvature at the two stations before rotor 1 L.E.

The predicted spanwise variation of C_m at L.E. stator 1 is lower than experimental variation and at hub and tip regions the velocity profile tends upwards. This may be due to assumption of constant polytropic coefficient. This discrepancy can be checked by running the program with actual value of polytropic coefficient at hub and tip. The differences between spanwise variations of predicted and experimental absolute Mach number follows that of C_m as expected. The L.E. conditions of stator 1 are taken to be same as those at trailing edge (T.E.) of rotor 1. Hence the total temperature and pressure ratio variations are lower than the experimental variations.

At L.E. of Rotor 2, the C_m profile is lower than experimental profile, Spanwise variation of other flow properties follows this trend. The total temperature and pressure ratios spanwise variations follows those of meridional velocities at L.E. of rotor 2 and stator 2.

IV.B. Five-Stage Transonic Axial-Flow Compressor (Reference 27) :-

This compressor was designed with all rotors operating with transonic relative inlet Mach numbers. The compressor was designed for radially constant axial velocity and other parameters. Inlet hub-to-tip ratio was 0.5 and exit hub-to-tip ratio was 0.816. No inlet guide vanes are used. The stators were designed to turn the air axially. Both rotor and stator blade sections were double-circular arc (DCA) profiles.

The computing time taken on IBM 370/165 Computer for the execution of entire performance map is 4 minutes. For a typical point near design condition, the computing time is 20 seconds.

IV.B.1 Overall Performance :-

The overall performance data for the five-stage compressor are presented in figure 7. These data cover a range of corrected speeds from 70 to 100 percent design. The total or stagnation pressure ratios predicted by the present method are 5 to 10 percent lower than the experimental values. For this compressor a constant value of polytropic coefficient is used for all operating points. Hence this results in a flat curve for the adiabatic efficiency. As expected, the efficiencies are in close agreement. The predicted efficiencies are usually 2 to 3 points lower than the experimental values.

Overall performance of individual stages is not presented for this compressor.

IV.B.2 Spanwise Variation of Pertinent Parameters at Design Point :

The spanwise variation of performance parameters at design point for this compressors are presented along with experimental profiles in figure 8. The spanwise variation of other parameters follows that of C_m variation as expected and no inconsistency is observed in either predicted or experimental profiles. But for later stages the variation in other parameters does not follow that of C_m, since at these stages, these parameters are affected by the discrepancies between experimentals and predicted performance of first stages. This can be explained as follows

$$\text{Total enthalpy } H_{i,j} = H_{i-1,j} + \omega[(rC_x \tan\alpha)_{i,j} - (rC_x \tan\alpha)_{i-1,j}] \quad \ldots \text{ IV.8}$$

Hence the discrepancy in C_x values of first stages affect the value of H at later stages. Since H enters in calculation of other parameters, the differences between predicted and experimental values are pronounced in later stages.

IV.C. Two-Stage Subsonic Axial-Flow Turbine (Reference 28):-

The turbine, having an overall loading of 3.25 for the two stages, was fitted with aerofoil camber-line type blading. The base

profile shape was placed around a parabolic camber line with the position of maximum camber at 40 per cent of the chord from the leading edge. The annulus was flared, with hub/to-tip ratio falling more or less linearly from 0.8 at inlet to the first-stage stator to 0.66 at exit from the second-stage rotor.

The computing time taken on IBM 370/165 Computer for the execution of entire performance map is 2 minutes. For a typical point near design condition, the computing time is 10 seconds.

IV.C.1 Overall Performance :-

The overall performance data for two-stage turbine is presented in figure 9. These data are presented at four speeds, 50 percent (i.e. $N/\sqrt{T_o}$ = 132), 75 percent (i.e. $N/\sqrt{T_o}$ = 194),87.5 percent (i.e. $N/\sqrt{T_o}$ = 230) and 100 percent (i.e. $N/\sqrt{T_o}$ = 263) design speed. The adiabatic efficiencies are in good agreement with the experimental values, as to be expected. The total pressure ratios predicted by the present method are about 10 percent below the experimental values. Here the total pressure ratio is the ratio of total pressure at inlet to the turbomachine,to total pressure at exit of the turbomachine.

IV.C.2. Spanwise Variation of Pertinent Parameters at Design Point :-

These data are presented in figure 10. Experimental data are not available for comparison. For stator 1, rotor 1 and stator 2 the L.E. meridional velocity profile is approximately constant along the

span. Other parameters follow this trend. For rotor 2, the C_m variation at tip is marked. Frost[20] had observed same trend at 87.5 percent design speed.

From the above discussions, it is observed that the spanwise variation of various parameters closely follows that of meridional velocity. Once the discrepancies between predicted and experimental C_m values are explained, differences in other parameters can easily explained. The reason for the discrepancies in C_m may be due to assumption of radially constant polytropic coefficient among other factors. This can be confirmed, if the program is run with variable polytropic coefficient.

CHAPTER V

CONCLUSIONS

A computer program for predicting the performance of turbomachines has been written. This has been done by taking calculating stations after blade rows and solving for axial velocity and streamline radius.

The following turbomachines have been selected as test cases for the program; a two-stage transonic axial-flow fan, a five-stage transonic axial-flow compressor and a two-stage subsonic axial-flow turbine.

The program predictions have been compared with experimental data, except for two-stage turbine.

The results obtained by the use of the present program are useful as a first approximation to determine the performance of turbomachines. The computed overall pressure ratios agree to within 5 percent of the experimental values in almost all cases tested. For compressors, the approach of stall is correctly predicted by the computed performance map, which is a useful feature.

The comparisons with the experiment show that this method gives a reasonable estimate of spanwise distribution of flow properties. An improvement on the measure of agreement demands a better model for the representation and distribution of losses.

The program was not run over a sufficiently wide range of parameters such as $N, {}_1, {}_2$ etc., to determine effect of these parameters.

SUGGESTIONS FOR FURTHER WORK:

In the present study, the polytropic coefficient is assumed to be constant at all grid points. This means that losses are equal at all streamlines. This assumption is invalid, since in hub and tip regions losses are more than in mid-span region of the blade. Hence, variable polytropic coefficient may be used to obtain more realistic performance data.

Swan[3] developed correlation of loss parameter with equivalent diffusion factor D_{eq} for D.C.A. rotor blade elements as a function of the percent of the span. These correlations may be extended to other types of blade and used in the present study. Then polytropic coefficient need not be fed in as input.

For transonic compressors, shock losses may be significant. In the present study, these losses are neglected. In further work, shock losses may be taken into account assuming the normal shock model developed in reference 30.

Hill and Lewis[31] has recently demonstrated that sweep and dihedral of the blades can very significantly affect cascade characteristics. Smith and Yeh[32] have already developed a model for including the above effects. The present program could be improved by incorporating suitable corrections.

In the present study, the relative fluid angles at off-design conditions are determined using correlation of deviation angles with equivalent diffusion factor. To obtain more realistic cascade characteristics an analytical cascade model should be developed and included in the present program.

In all mathematical models of turbomachine flow field, the formulation starts with inviscid fluid assumptions, but losses are introduced by means of a polytropic coefficient or pressure loss coefficient. Smith[5] had reservations about this approach. Horlock[22] had taken into account of this fact and formulated the problem starting with viscous flow equations. Bosman and Marsh[21] had included this correction in their formulation for matrix through flow method. The present formulation may be modified in those lines. Finally any theoretical method should be compared with other theoretical methods. Hence the results of this program may be compared with those of references 19,20 and 21.

REFERENCES

1. Wu C.H., 'A general theory of three-dimensional flow in subsonic and supersonic turbomachines of axial, radial and mixed-flow types', N.A.C.A. TN 2604, 1952.

2. Serovy G.K. and Anderson D.W., 'Method for predicting off design performance of axial-flow compressor blade rows', NASA TN D-110, 1959.

3. Swan W.C., 'A practical method of predicting transonic axial-flow compressor performance', Journal of Engineering for Power, Trans. ASME, Series A, 1961, 83, 322-330.

4. Holmquist C.O. and Mannie W.D., 'An approximate method of calculating three-dimensional compressible flow in axial turbomachines', Journal of the Aeronautical Sciences, 1956, 23, 543-556.

5. Smith L.H., 'The radial equilibrium equation of turbomachinery', Journal of Engineering for Power, Trans. ASME, Series A, 1966, 88, 1-12.

6. Hawthorne W.R. and Novak R.A., 'Aerodynamics of turbomachinery', Annual Review of Fluid Mechanics, Vol.1, 1969, 341-366.

7. Moorthy C.S., 'Axi-symmetric flow with application to axial-flow turbomachines', Journal of the Aeronautical Society of India, 1967, 19(1), 1-15.

8. Silvester M.E. and Hetherington R., 'A numerical solution of the three-dimensional compressible flow through axial turbomachines', Numerical Analysis : an Introduction, Ed. J. Walsh, Academic Press, 1965.

9. Hamati C.C.Jr. and Finger H.B., 'Design velocity distribution in meridional plane', Ch. VIII, Aerodynamic Design of Axial-Flow Compressors NASA SP-36, Eds.I.A. Johnsen and R.O. Bullock, 1965.

10. Bullock R.O. and Johnsen I.A., 'Compressor design system', Ch. III, Aerodynamic Design of Axial-Flow Compressors, NASA SP-36, Eds. I.A. Johnsen and R.O. Bullock, 1965.

11. Janzen W. and Moffatt W.C., 'The off design analysis of axial flow compressors', Journal of Engineering for Power. Trans. ASME Series 89, 453-462.

12. Novak R.A., 'Streamline curvature computing procedures for fluid flow problems', ibid, 478-490.

13. Crevilling H.F. and Darmody R.H., 'Axial-flow compressor computer program for calculating off-design performance (Program IV), NASA CR-72427, 1968.

14. Daneshyar H. and Shalaan M.R.A., 'The off-design analysis of flow in axial-flow compressors', ARC CP 1234, 197

15. Marsh H., 'The uniqueness of turbomachinery flow calculations using the streamline curvature and matrix thro

flow methods', Journal of Mechanical Engineering Science, 1971, 13(6), 376-385.

16. Wilkinson D.H., 'Stability and convergency of two-dimensional streamline curvature methods using quasi-orthogonals', Institute of Mechanical Engineers Thermodynamics and Fluid Mechanics Convention, Paper 35, 1970.

17. Mazumdar A.S., 'A review of recent computational procedure for off design analysis of axial compressors', Journal of Aeronautical Society of India, 1975, 27(1), 8-16.

18. Davis W.R., 'A computer program for the analysis and design of turbomachinery - Revision', Carleton University Report ME/A-71-5, 1971.

19. Marsh H., 'A digital computer program for the through-flow fluid mechanics in an arbitrary turbomachine using a matrix method', ARC R&M 3509, 1968.

20. Frost D.H., 'A streamline curvature through-flow computer program for analysing the flow through axial-flow turbomachines', ARC R&M 3687, 1972.

21. Bosman C. and Marsh H., 'An improved method for calculating the flow in turbomachines, including a consistent loss model', Journal of Mechanical Engineering Science, 1974, 16(1), 25-32.

22. Horlock J.H., 'On entropy production in adiabatic flow in turbomachines', Journal of Basic Engineering, Trans. ASME, Series D, 1971, 93.

23. Flagg J.F., 'Analytical procedure and computer program for determining the off-design performance of axial flow turbines', NASA CR-710, 1967.

24. Renaudin B. and Somm F., 'Quasi three dimensional flow in a multistage turbine-calculation and experimental verification', Flow Research on Blading, Ed. L.S. Dzung, Elsevier Publishing Company, 1970.

25. Ribaut M., 'Three-dimensional calculation of flow in turbomachines with the aid of singularities', Journal of Engineering for power, Trans. ASME, Series A, 1968, 90, 258-264.

26. Ruggeri R.S. and Benser W.A., 'Performance of a highly loaded two-stage axial-flow fan', NASA TM X-3076, 1974.

27. Kovach K. and Sandercock D.M., 'Aerodynamic design and performance of five-stage transonic axial-flow compressor', Journal of Engineering for Power, Trans. ASME, Series A, 81, 1961.

28. Johnson I.H. and Smart D.E., 'An experiment in turbine blade profile design, ARC CP 941, 1965.

29. Walsh J.L., and Nilson E.N., 'Best approximation properties of the spline fit', Journal of Mathematics and Mechanics, 1962, 11, 225-234.

30. Miller G.F., Lewis G.W. Jr., and Hartmann M.J., 'Shock losses in transonic compressor blade rows', Journal of Engineering for Power, Trans. ASME, Series A, 1961, 83.

31. Hill J.M. and Lewis R.I., 'Experimental investigations of strongly swept turbine cascades with low speed flow', Journal of Mechanical Engineering Science, 1974, 16(1) 32-40.

32. Smith L.H. and Yeh H., 'Sweep and dihedral effects in axial-flow turbomachinery', Journal of Basic Engineering, Trans. ASME, Series D, 1963, 85, 401-416.

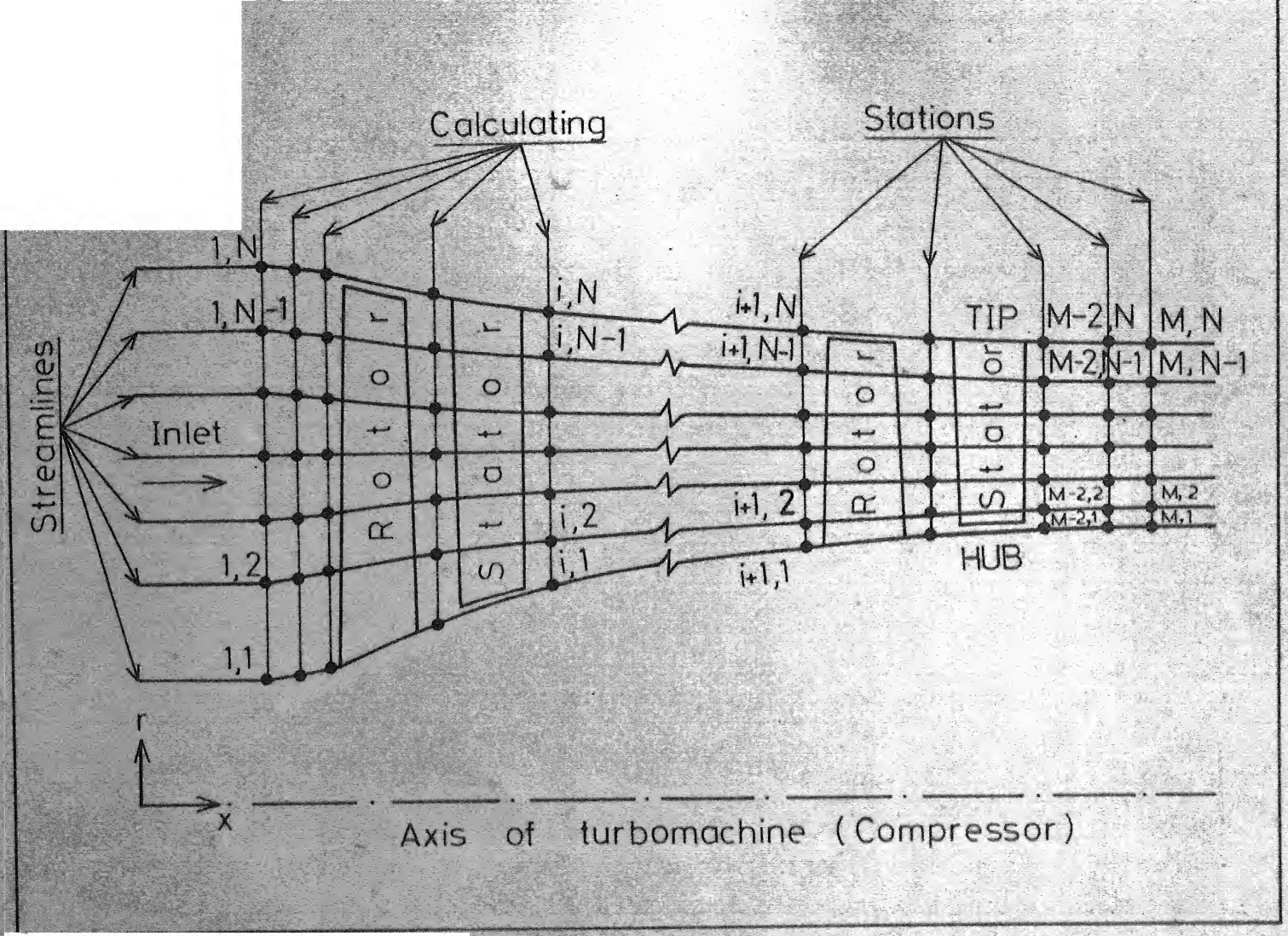

Fig.1. meridional plane of axial-flow turbomachine(Compr
grid .

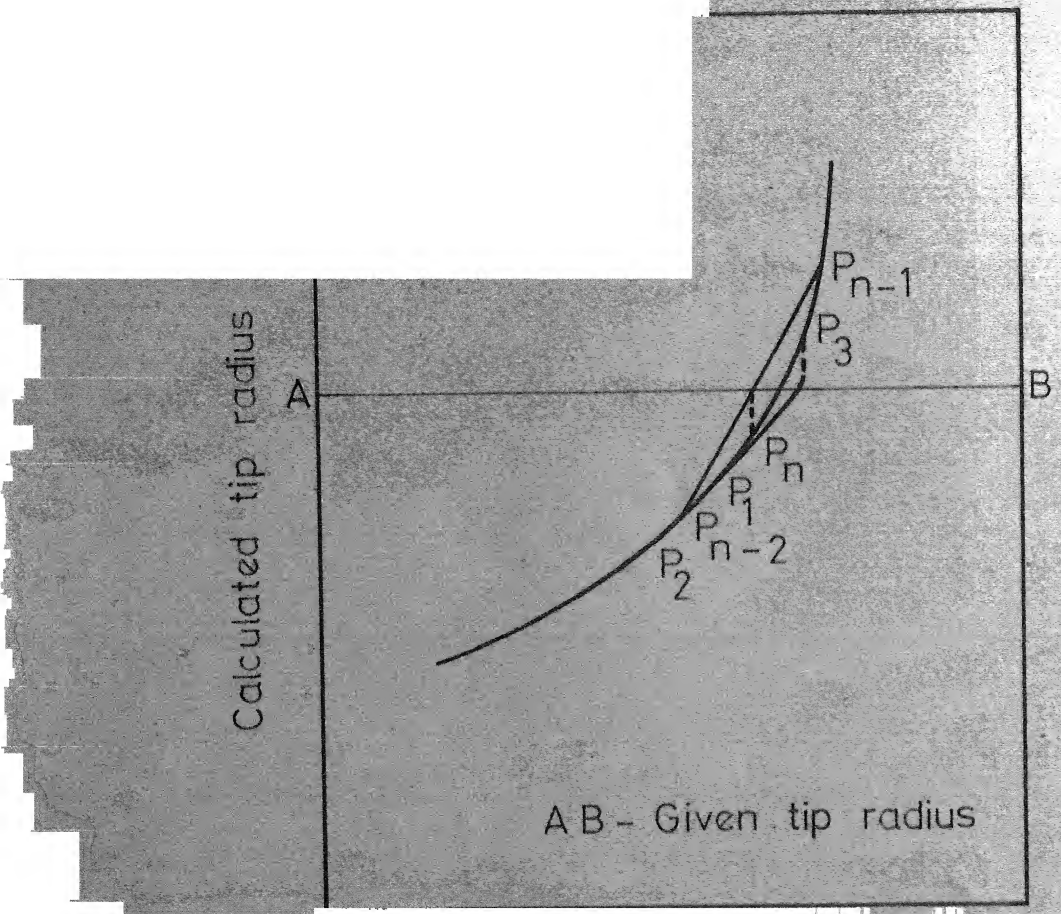

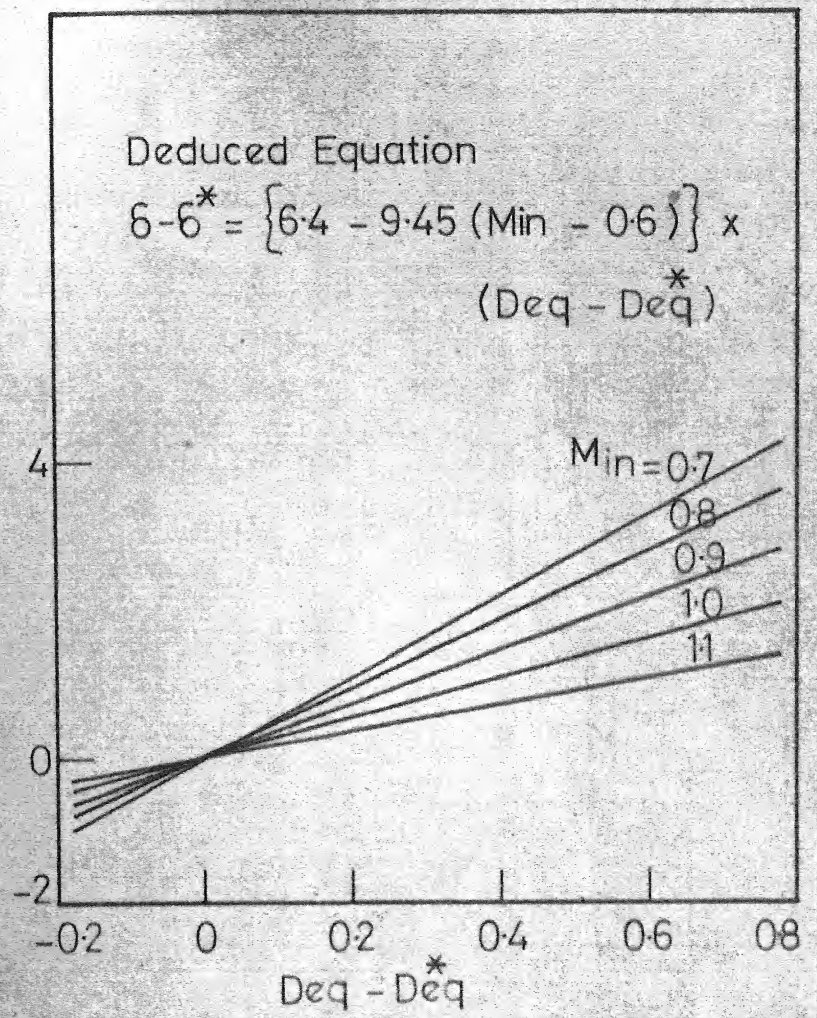

FIG. 3 - OFF MINIMUM LOSS VARIATION OF DEVIATION ANGLE WITH E DIFFUSION FACTOR FOR D.C.A ROTOR BLADE ELEMENTS.

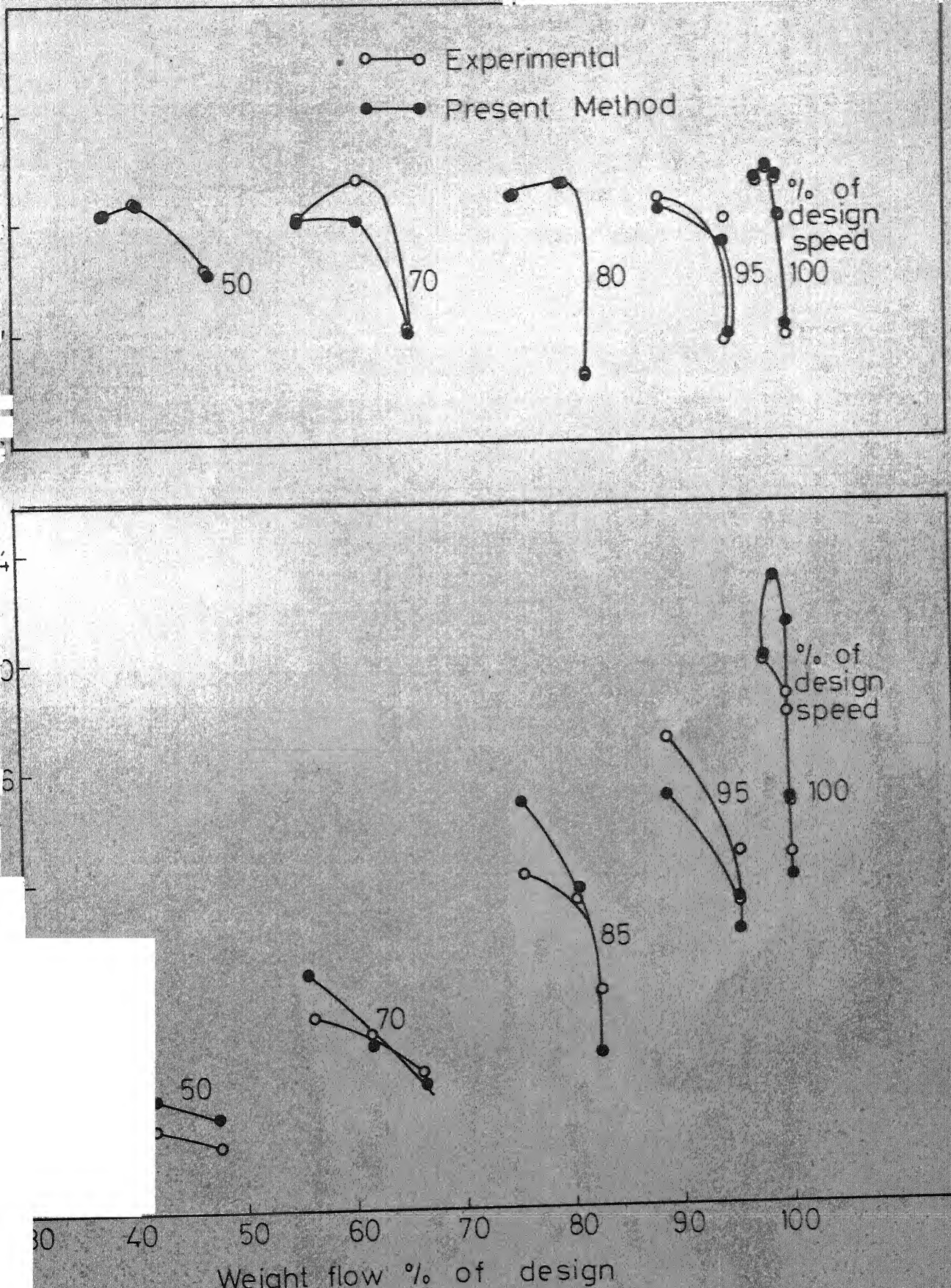

Fig. 4. Overall performance of two-stage transonic axial-flow fan (Reference 26)

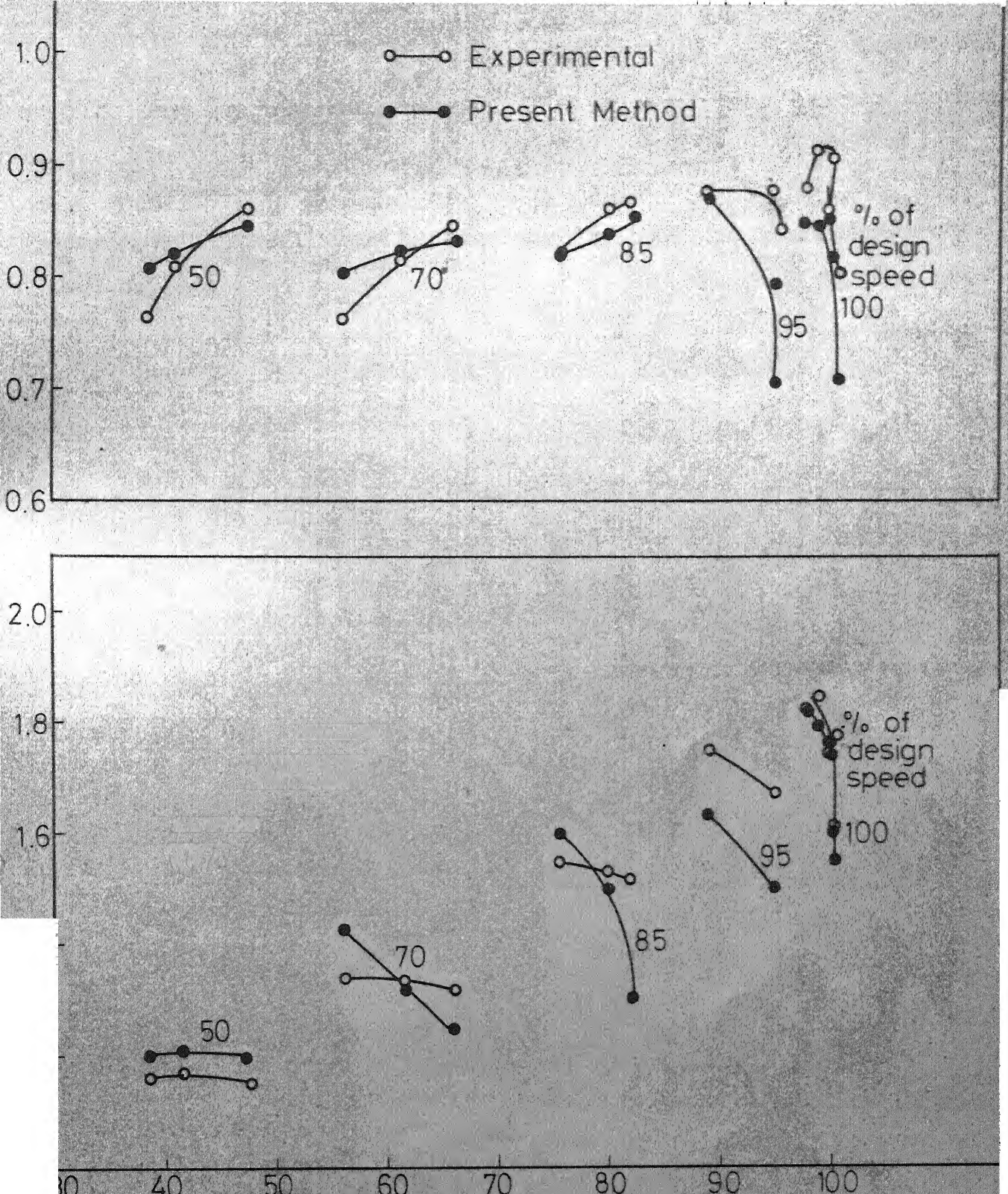

Fig. 5 First stage performance of two stage fan (Reference 26)

β at L.E. Degrees
70
60
50
Pressure ratio
1.8
1.6
Temp. ratio
1.20
1.18
1.16
0
20
40
60
80
100
Radial location, % of span
(a) Rotor 1

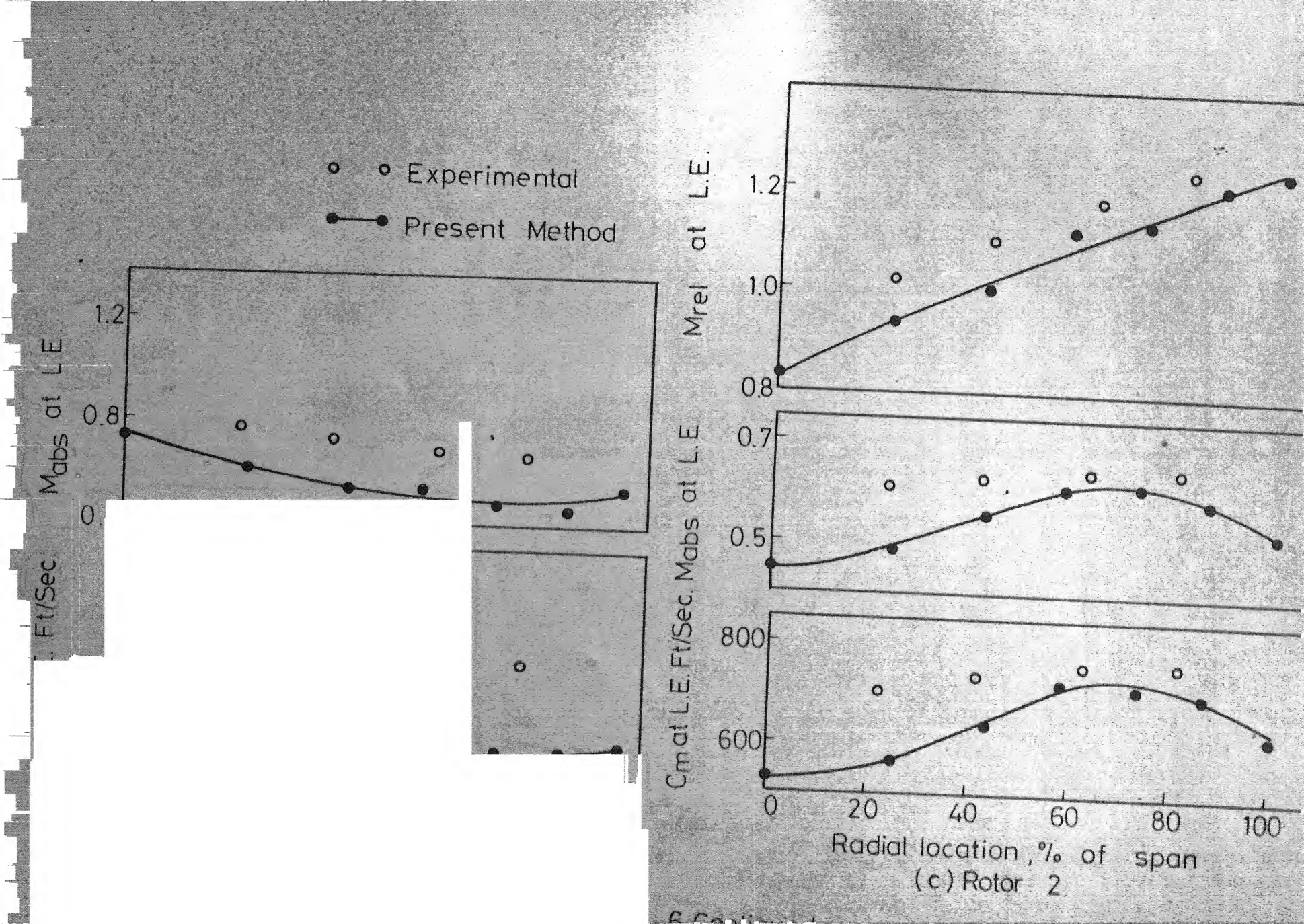
Experimental
Present Method
Mabs at L.E
1.2
0.8
0
Ft/Sec
Mrel at L.E.
1.2
1.0
0.8
Cm at L.E. Ft/Sec. Mabs at L.E
0.7
0.5
800
600
0
20
40
60
80
100
Radial location, % of span
(c) Rotor 2

Experimental
Present Method
Mabs at L.E.
0.8
0.6
Cm at L.E Ft/Sec
800
600
0
20
40
60
80
100
Radial location, % of span
(d) Stator 2
3.0
2.6
2
1.3

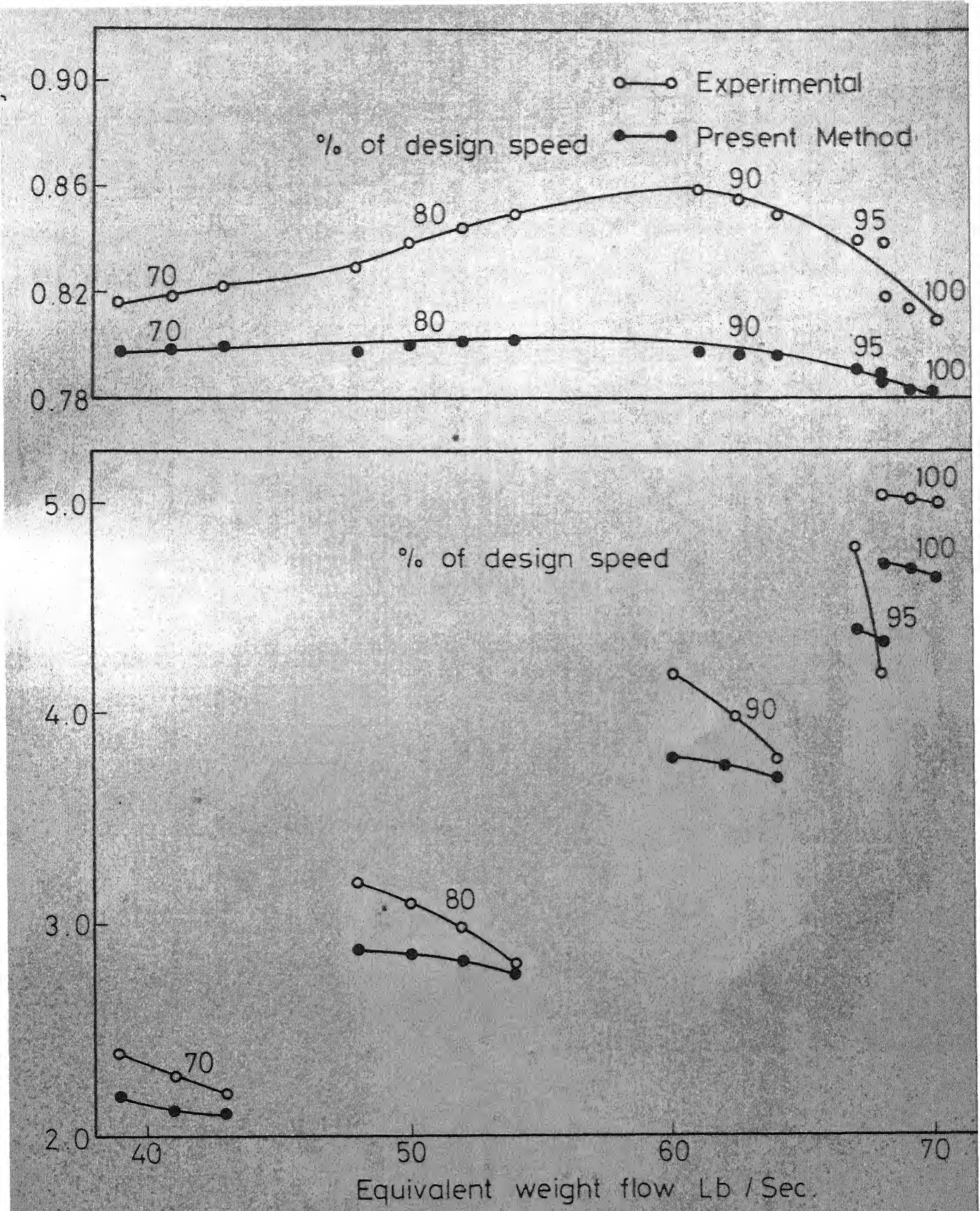

g.7 Overall performance of five-stage transonic axial flow compres
(Reference 27)

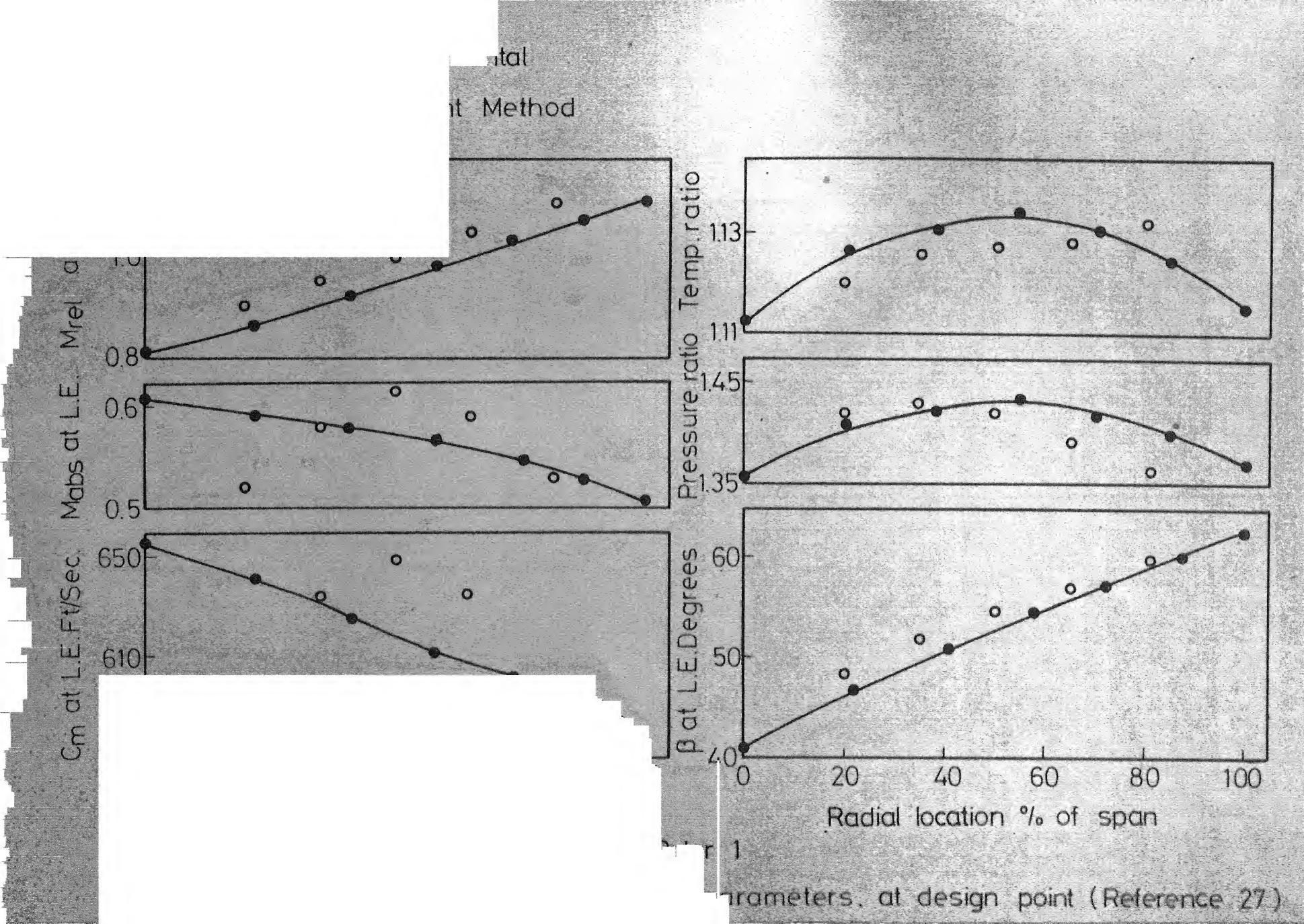

ıtal

ıt Method

r 1

rameters, at design point (Reference 27)

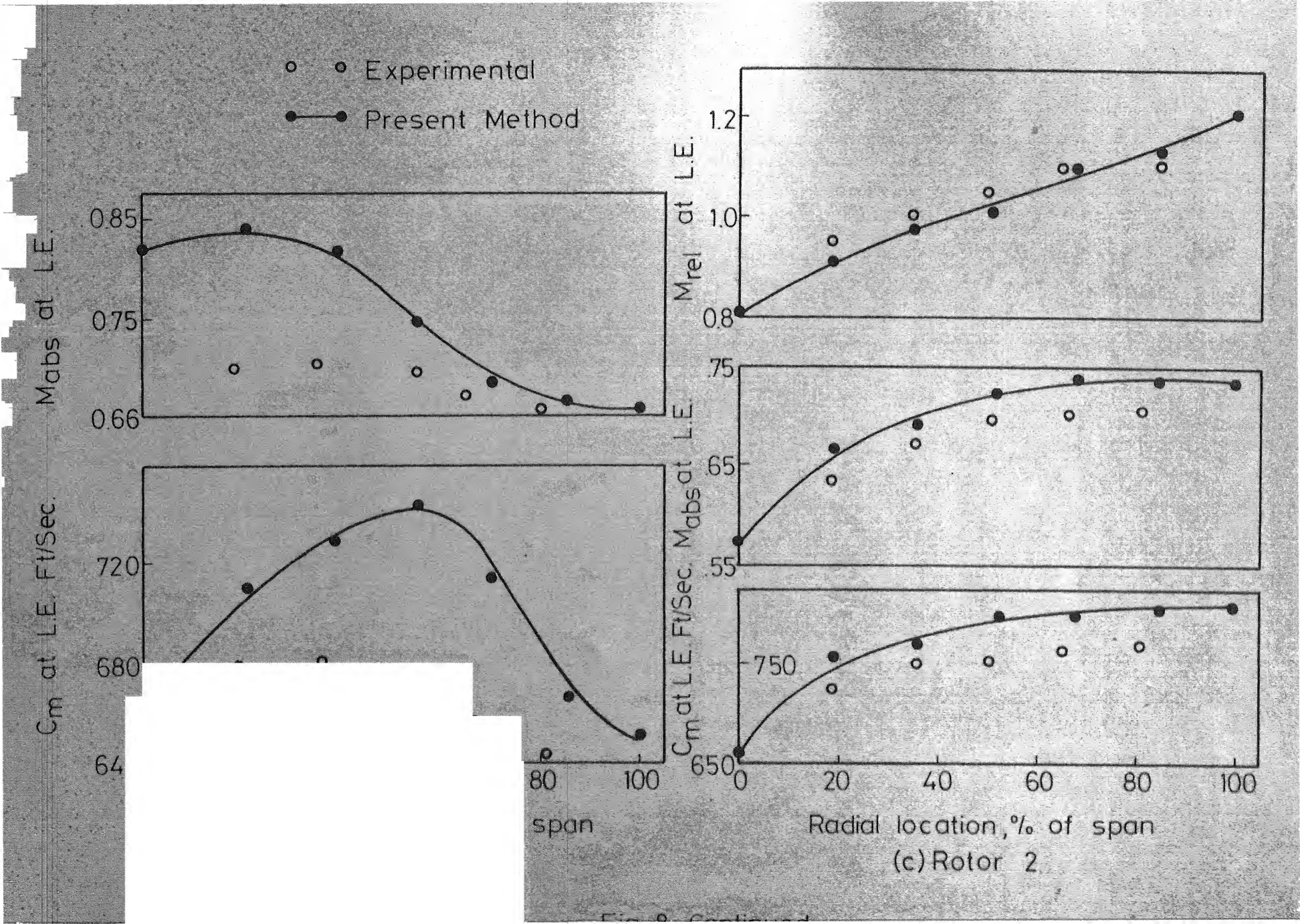
Experimental
Present Method
Mabs at L.E.
0.85
0.75
0.66
Cm at L.E. Ft/Sec.
720
680
64
80
100
span
Mrel at L.E.
1.2
1.0
0.8
Cm at L.E. Ft/Sec. Mabs at L.E.
.75
.65
.55
750
650
0
20
40
60
80
100
Radial location, % of span

(c) Rotor 2

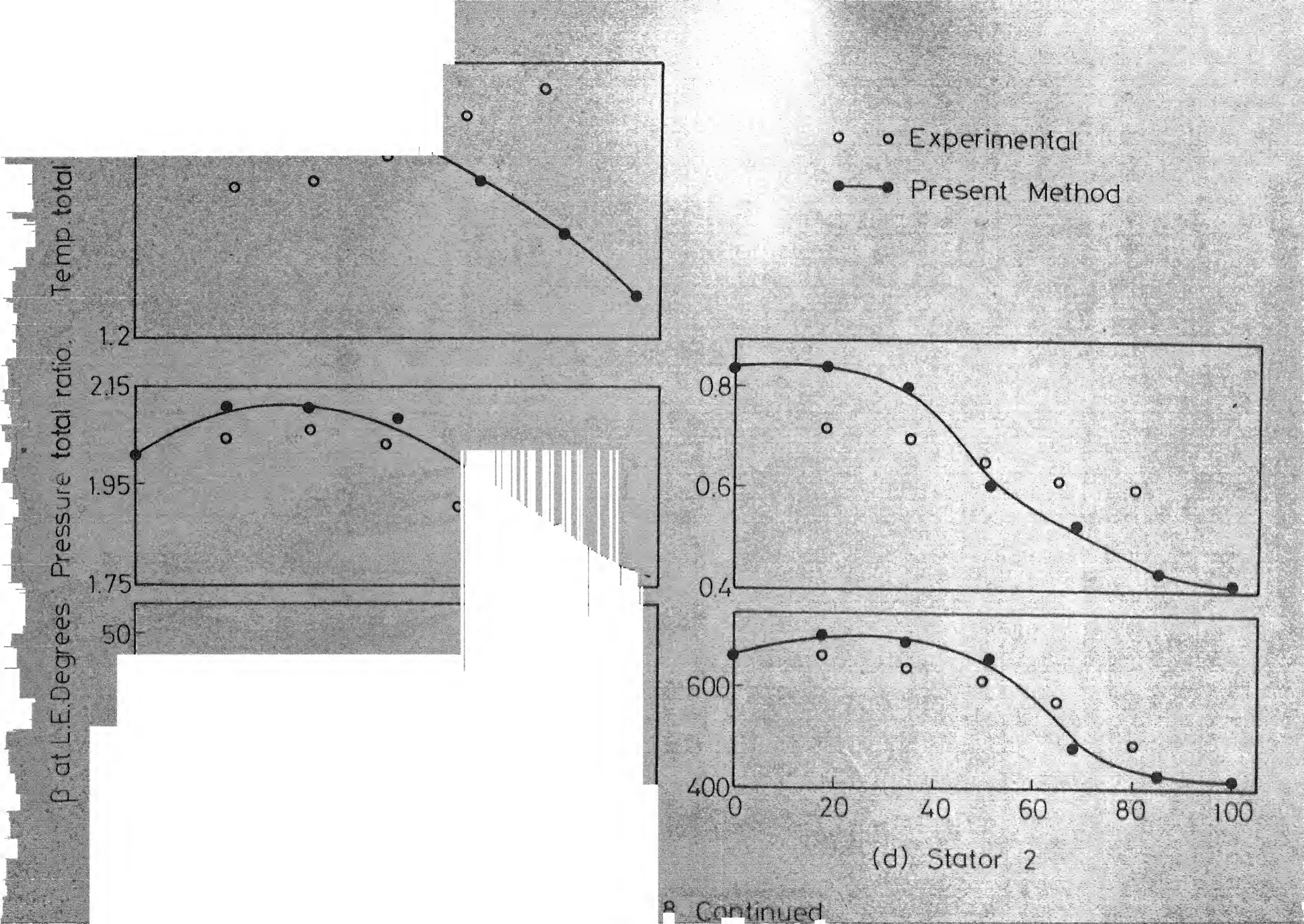

(d) Stator 2

Continued

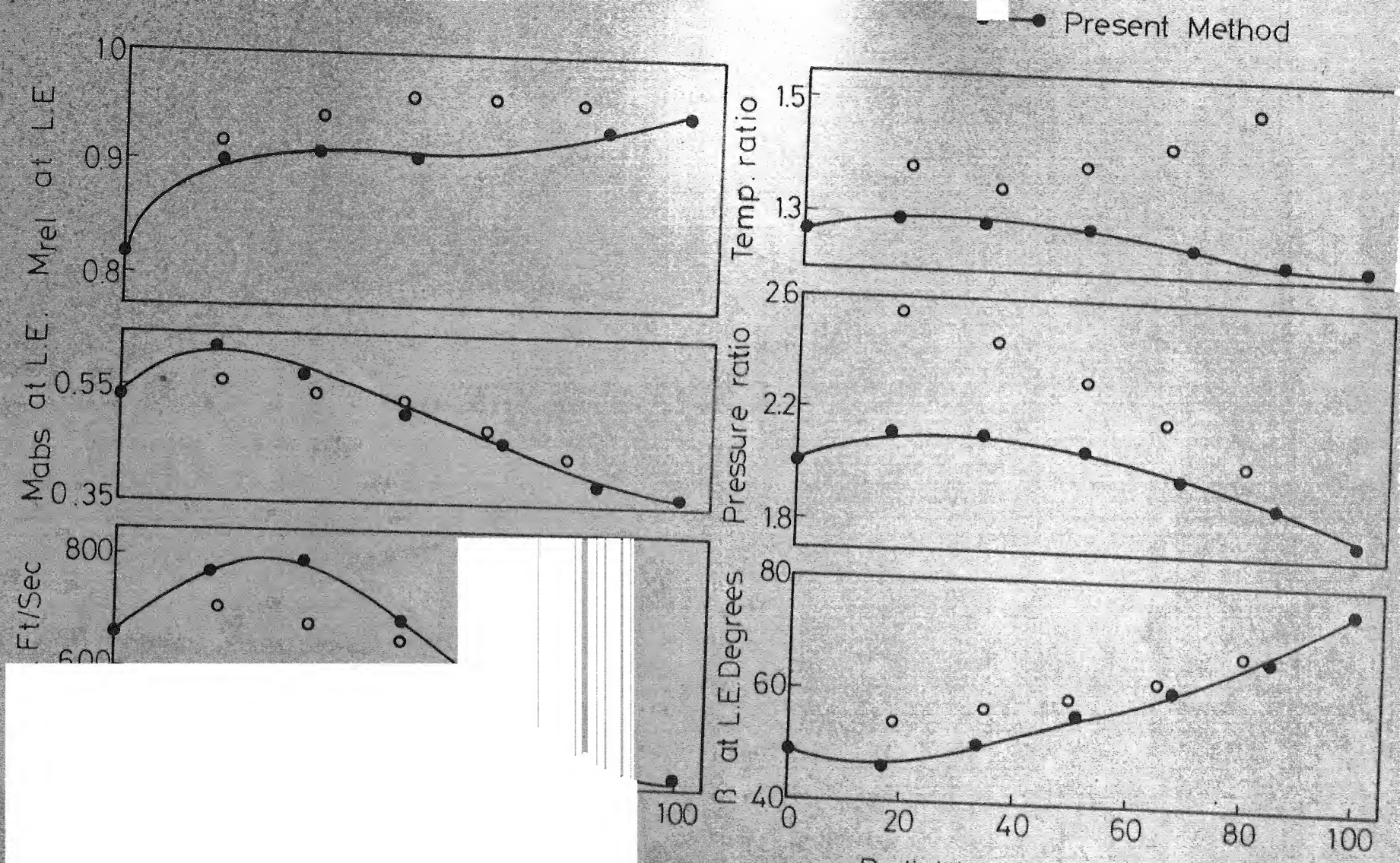

(e) Rotor 3

8 Continued

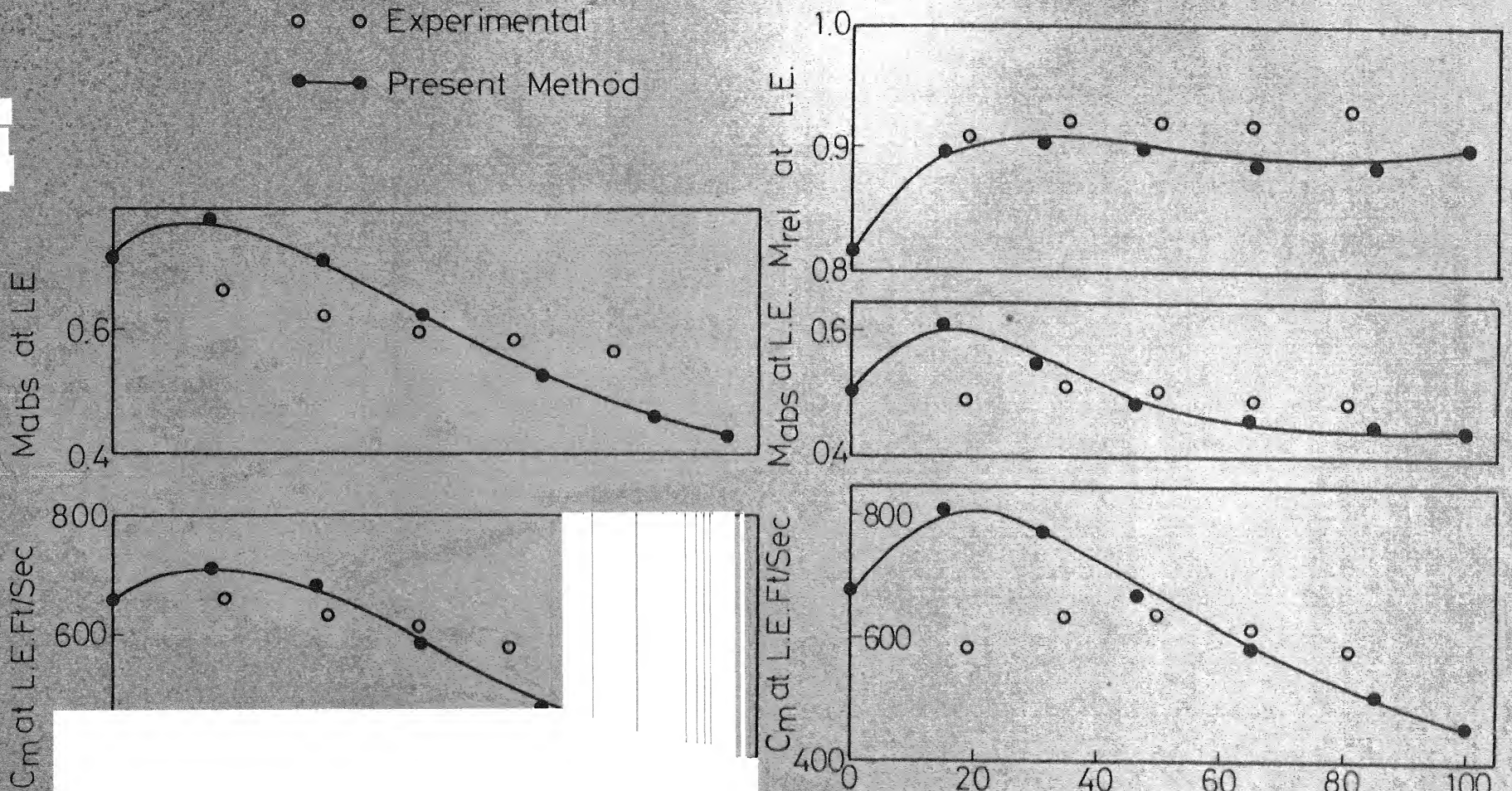

(g) Rotor 4

Continued

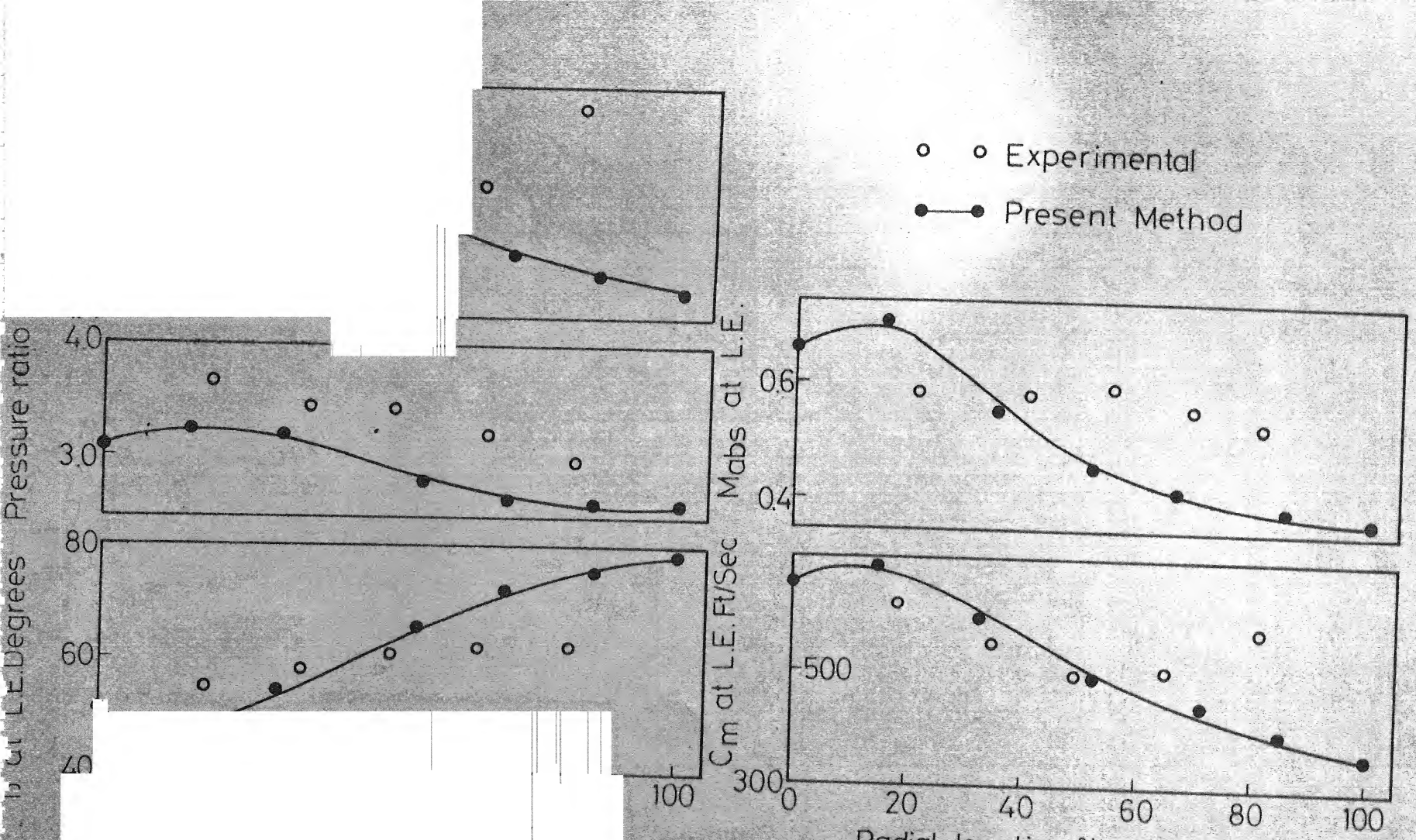

(h) Stator 4

g. 8. Continued

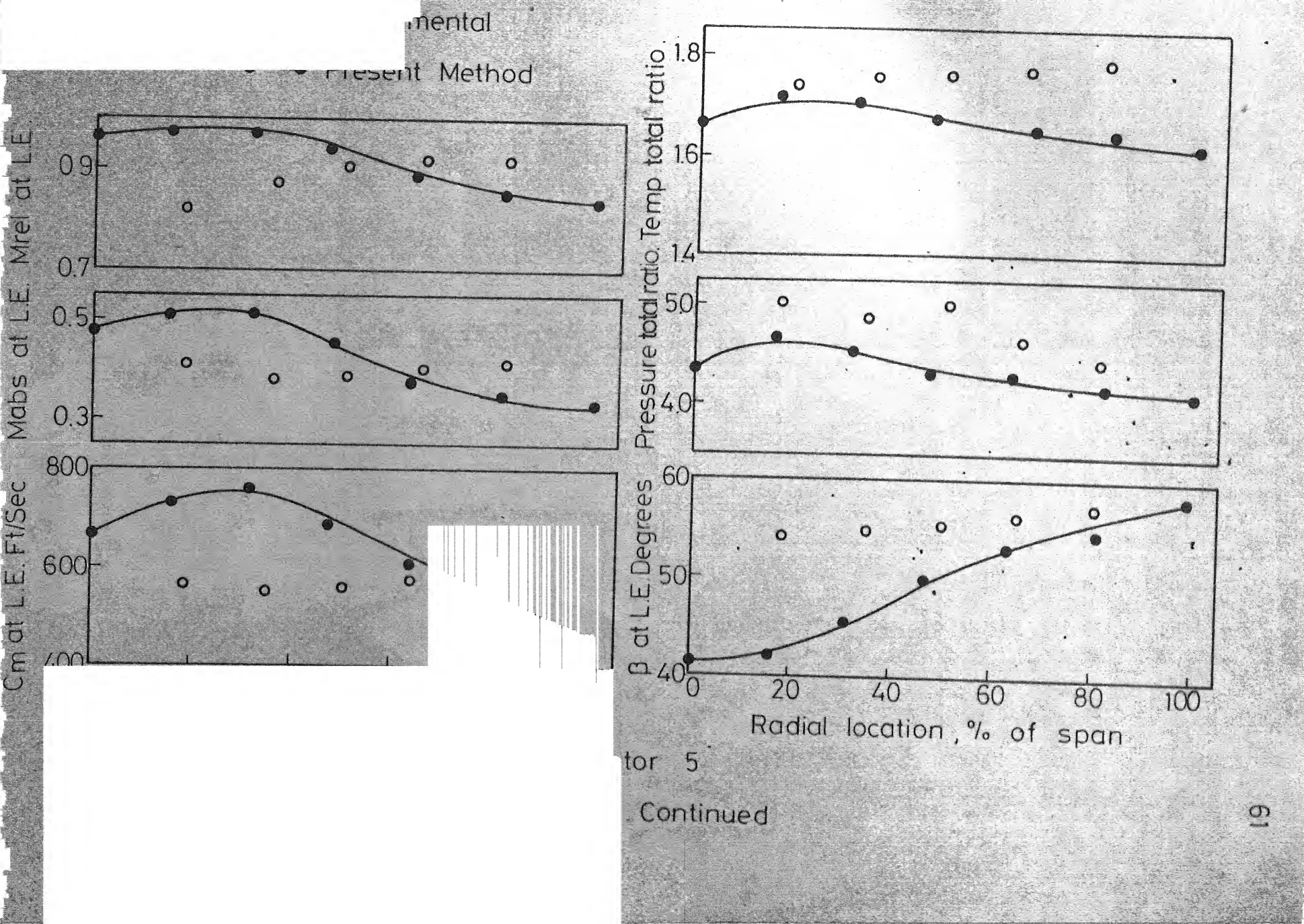

tor 5

Continued

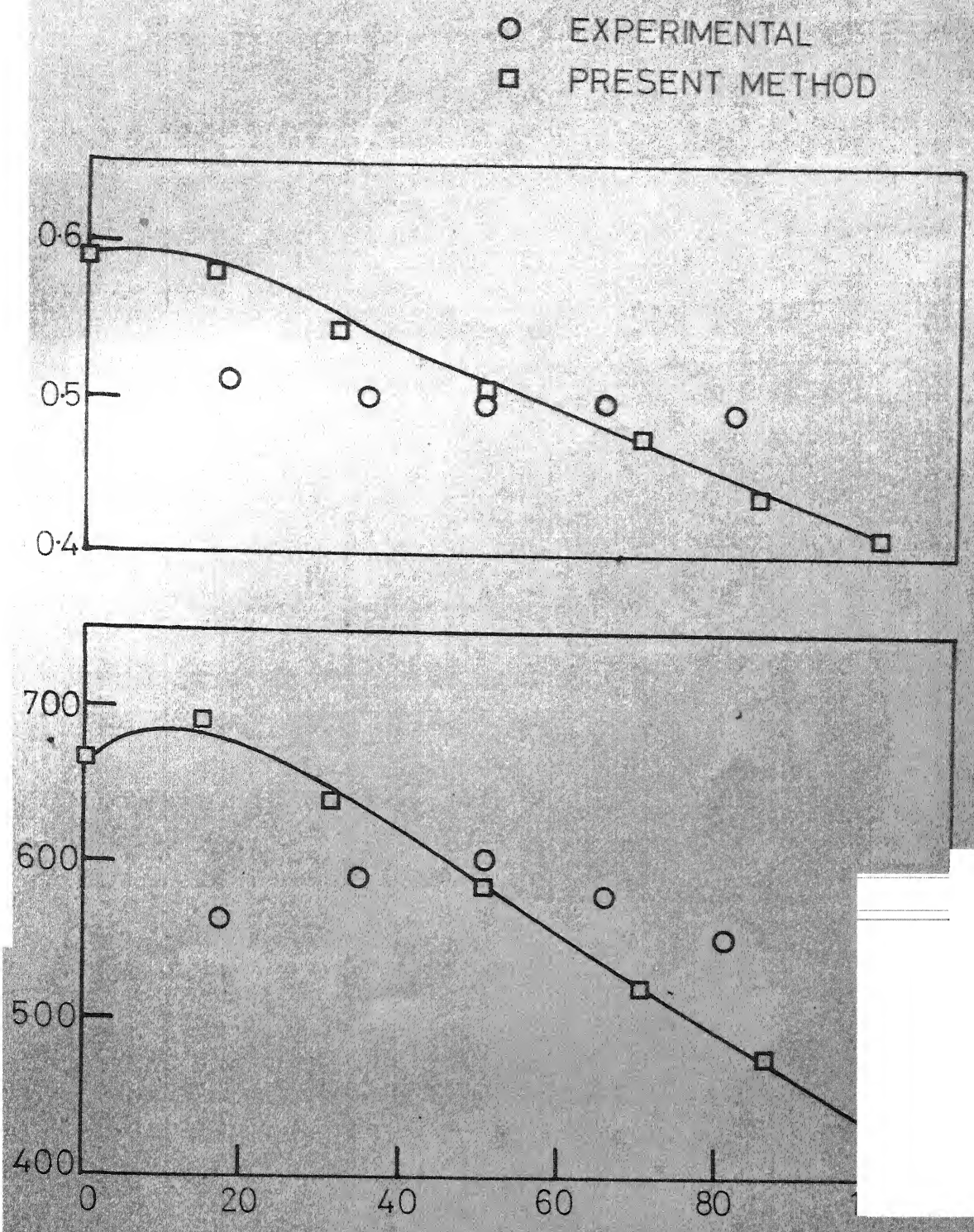

j) Stator 5

FIG. 8 - CONCLUDED

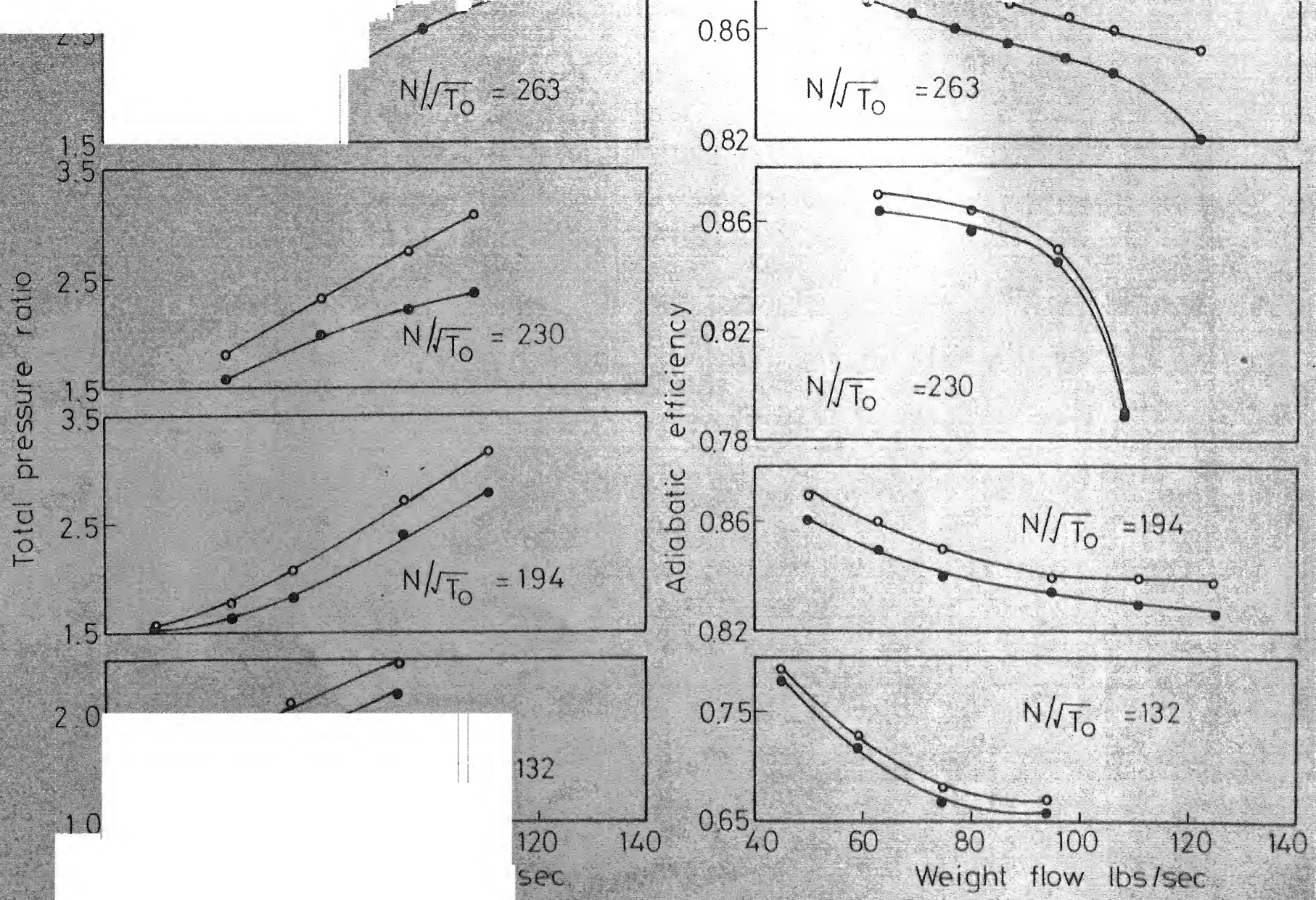

two - stage subsonic axial - flow turbine (Reference

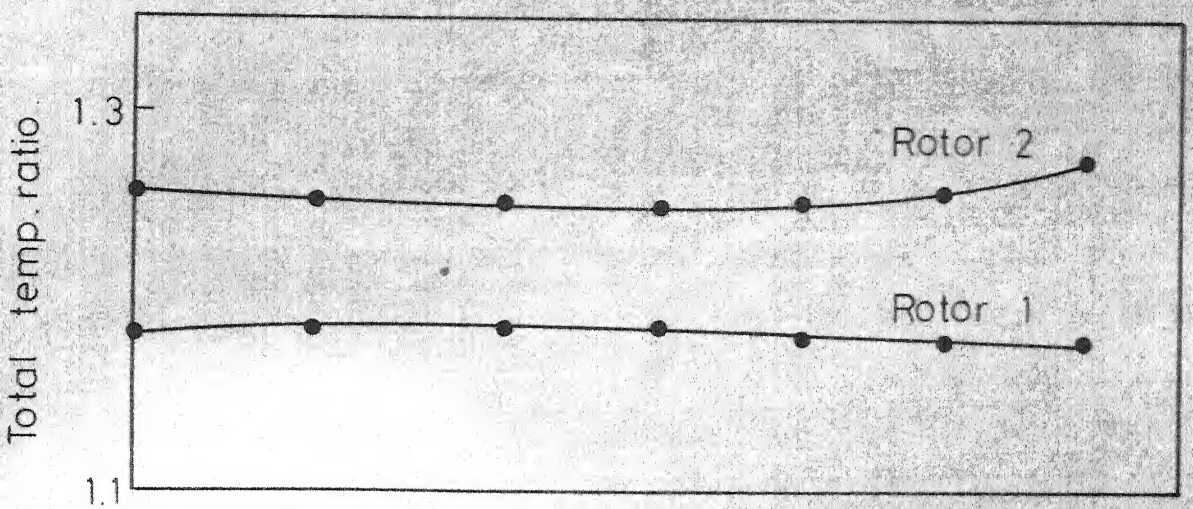

(f) Total temperature ratio distribution

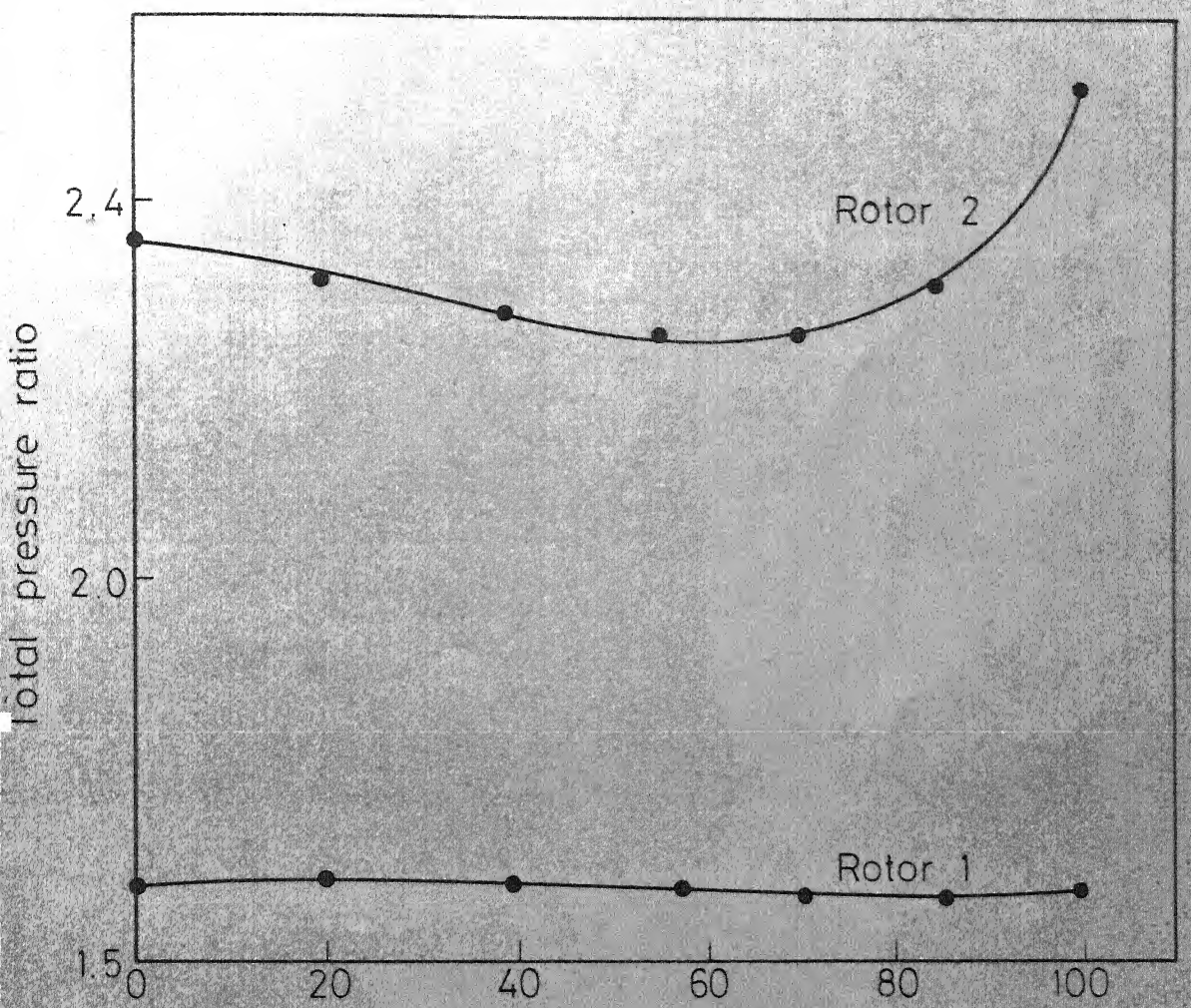

(e) Pressure ratio distribution

Fig. 10. Concluded

AE-1975-M-SIT-PER

This book is to be returned on the date last stamped.

.....	.....
.....	.....
.....	.....
.....	.....
.....	.....
.....	.....
.....	.....
.....	.....
.....	.....
.....	.....
.....	.....

CD 6.72.9